Anita Leitgeb

Towards Latent Olefin Metathesis Catalysts: The Use of 2-Vinylbenzamides as Carbene Precursors

DIPLOMA THESIS

Diplomarbeit

zur Erlangung des akademischen Grades einer
Diplom-Ingenieurin

der Studienrichtung Allgemeine Technische Chemie
erreicht an der Technischen Universität Graz

Oktober 2008

Betreuer: Univ.-Doz. Dipl. Ing. Dr. techn. Christian Slugovc
Institut für Chemische Technologie von Materialien
Technische Universität Graz

FIANT CRISTALLI

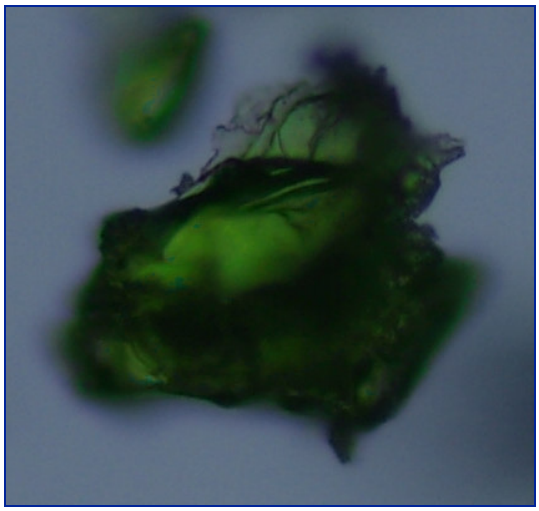

"Experience is not what happens to a man; it is what a man does with what happens to him."

Aldous Huxley (1894-1963)

Acknowledgement

I express my deep gratitude to all those who supported my diploma thesis, and those, who accompanied me in my studies:

I thank Prof. Christian “Slugi” Slugovc for supervising my diploma thesis, for giving me the opportunity of participating at international conferences and for an inspirational atmosphere at work.

I thank Prof. Franz Stelzer for the opportunity to do this work at ICTM.

My gratitude also goes to Dr. Petra Kaschnitz and the “NMR – team”, Prof. Kurt Mereiter and Prof. Robert Saf and his team for all the measurements.

Thanks to Jon David Andrade from Brown University for the synthesis of some ligands.

I thank all my colleagues at ICTM and my friends for fruitful discussions and many happy hours in – and outside the lab. Special thanks to Gabi, Achim, Michi, Thommy, Lexi, Fab and Babsi. You are great!

Financial support by “Technische Universität Graz” (Förderstipendium), by the Austrian Science Fund (FWF) and Umicore AG is gratefully acknowledged.

I am most grateful to my parents for supporting me at all times and in all respects, for their confidence in me, for being encouraging and understanding.

Abstract

Recent developments in organic electronics such as OLEDs (organic light emitting devices) or photovoltaic devices have opened a wide field of research in many areas of physics and chemistry. The growing potential of high – tech – polymers has greatly increased the need for tailored transition metal complexes initiating ROMP (ring opening metathesis polymerization). These initiators have to comply with specific demands such as high functional group tolerance, “livingness” and a high polymerization rate. A new challenge is posed by the claim for so called dormant metathesis initiators for special applications such as ink jet printing. It is aimed to get catalysts that can be mixed and stored together with the monomer without initiating any reaction beneath a certain triggering temperature.

In this work, the synthesis and characterization of a new type of latent ruthenium complexes bearing chelating carbene ligands based on the amide function is presented. Different secondary and tertiary benzoic acid derived amides have been synthesized and used as ligands of Grubbs – type ruthenium complexes. Structural analysis concerning the stoicheometry and stereochemistry of the obtained complexes was done by NMR (nuclear magnetic resonance) spectroscopy, X-ray diffractometry and MALDI – TOF – MS (matrix assisted laser deposition ionization – time of flight – mass spectrometry).

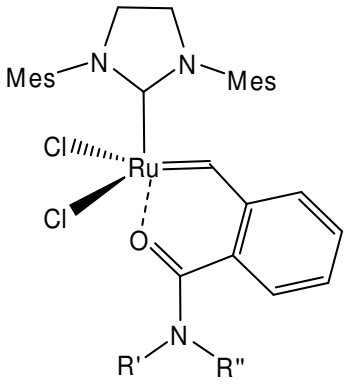

Zusammenfassung

In den letzten Jahren haben Entwicklungen im Bereich der organischen Elektronik (z. B. OLEDS (organic light emitting devices) oder Solarzellen) ein breites Forschungsfeld in vielen Bereichen der Physik und der Chemie eröffnet. Das wachsende Potential von High-Tech-Polymeren hat die Nachfrage nach maßgeschneiderten Übergangsmetallkomplexen welche als Initiator für ROMP (Ring öffnende Metathese Polymerisation) verwendet werden können, dramatisch erhöht. Solche Initiatoren müssen speziellen Anforderungen wie hohe Toleranz gegenüber funktionellen Gruppen, die Möglichkeit von lebender Polymerisation sowie hohe Polymerisationsraten gerecht werden. Eine neue Herausforderung bildet die Nachfrage nach so genannten „schlafenden" Metatheseinitiatoren für spezielle Anwendungen wie z.B. Ink Jet Printing. Das Ziel ist es, Initiatoren herzustellen, welche zusammen mit dem Monomer gelagert werden können ohne dabei unter einer definierten, Schalttemperatur die Polymerisation zu starten.

In dieser Arbeit werden Synthese und Charakterisierung eines neuen Typs latenter Rutheniumkatalysatoren mit chelatisierenden Carbenliganden, welche eine Amidgruppe tragen, vorgestellt. Es wurden verschiedene sekundäre und tertiäre Benzoesäureamide hergestellt und als Liganden für Rutheniumkomplexe des Grubbs – Typs verwendet. Mittels NMR (Nuclear Magnetic Resonance) – Spektroskopie, Röntgendiffraktometrie und MALDI – TOF – MS (Matrix Assisted Laser Deposition Ionization – Time Of Flight – Massenspektrometrie) wurde strukturelle Analyse zur Aufklärung von Stöchiometrie und Stereochemie der erhaltenen Komplexe durchgeführt.

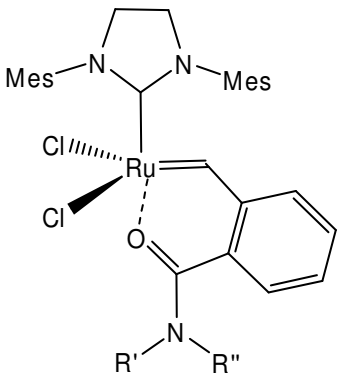

TABLE OF CONTENT

1 INTRODUCTION AND MOTIVATION

1.1 Thermally Triggered ROMP Initiators

In recent years the growing potential of specialty polymers has greatly increased the need for tailored transition metal complexes initiating ROMP (ring opening metathesis polymerization). Properties such as versatility, a high functional group tolerance, “livingness” and a high polymerization rate are demands that are already met by state-of-the-art-initiators. Another challenge is posed by the claim for thermally triggered metathesis catalysts for special applications.[1]

The following figure presents four different design motives that have been followed in order to create temperature dependant polymerization by using so called dormant or latent ruthenium carbene complexes.

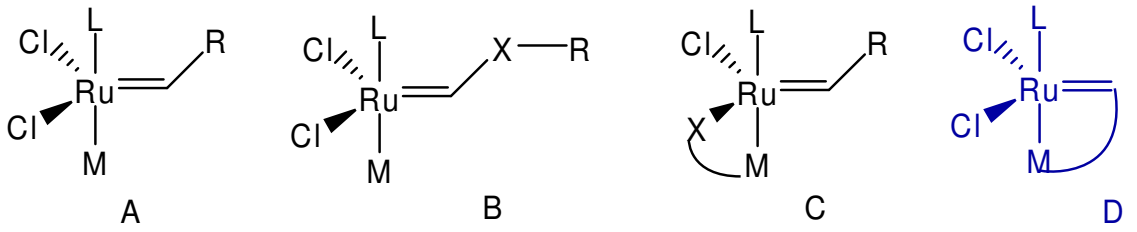

Fig. 1: Possible designs for a thermally switchable initiator

Motive A represents the Grubbs – type initiator bearing a Schrock carbene ligand. The idea is to use a ligand M which is strongly bonded to the Ruthenium centre and only cleaved off when exposed to elevated temperatures. So far, no such ligand has been found. In this special ligand environment of these particular complexes all ligands M (such as phosphines, amines etc.) are comparatively weakly bonded. In motive B, a Fischer carbene, formed through electron rich elements such as oxygen, sulphur or nitrogen hinders metathesis electronically.[2] Motive C has been followed by our working group during the last years using bidentate or tridentate ligands such as tris(pyrazolyl)borate.[3] Metathesis can only happen when a free coordination site at the ruthenium centre is established by decoordination of a ligand. Resulting competition

[1] Gstrein, X.; Burtscher, D.; Szadkowska, A.; Barbasiewicz, M.; Stelzer, F.; Grela, K.; Slugovc, C. *J. Polym. Sci.Part A: Polym. Chem*. **2007**, *45*, 3494-3500.
[2] Louie, J.; Grubbs, R. H. *Organometallics*, **2002**, *21*, 2153-2164.
[3] Burtscher, D.; Perner, B.; Mereiter, K.; Slugovc, C. *J. Organomet. Chem.* **2006** *, 691,* 5423–5430

between the approaching monomer and the recoordination of this ligand leads to undesirable slow propagation rates.

In contrast, motive D with its chelating carbene ligand enables fast propagation after the requested retarded initiation step and is therefore assumed to be the most promising concept for the realization of dormant initiators.

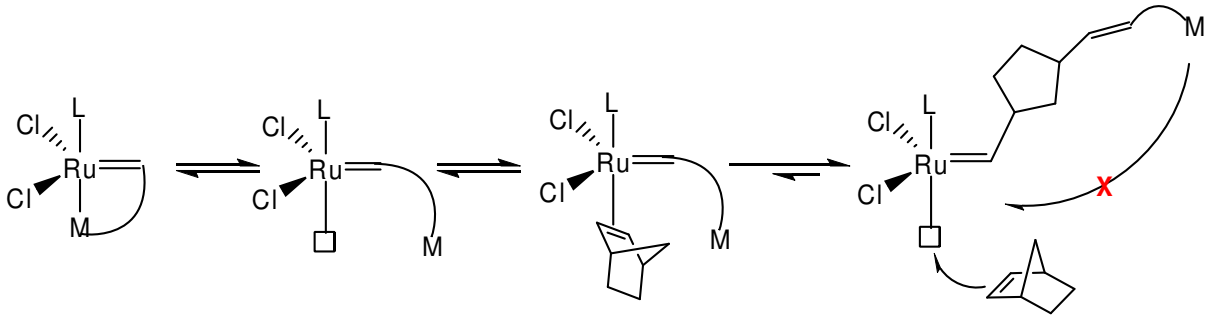

Scheme 1: Polymerization with an initiator of type D

In the last few years the development of such initiators has played a dominant role in the research of our group.[4,5] This work is another contribution to a better understanding of Ruthenium complexes bearing chelating carbene ligands. The main goals summarized in the following: The first step is the synthesis of several suitable ligands bearing a secondary or tertiary amide function. Subsequently, ruthenium complexes as described above should be synthesized. Different analysis methods such as NMR spectroscopy, mass spectroscopy and X-ray diffractometry should be applied to determine the exact structural features that are to be compared with analogue ester derivatives. The reactivity of the obtained complexes should be tested in ROMP and RCM experiments.

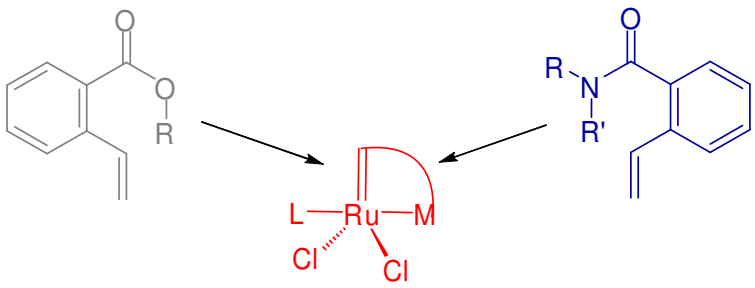

[4] Slugovc, C.; Burtscher, D.; Stelzer, F.; Merreiter, K. *Organometallics*, **2005**, *24*, 2255-2258
[5] Slugovc, C.; Perner, B.; Stelzer, F.; Mereiter, K. *Organometallics* **2004**, *23*, 3622-3626.

2 GENERAL BACKGROUND

2.1 Olefin Metathesis

Intensive research on transition metal complexes and their use in metathesis chemistry during the last 15 years has lead to enormous developments in organic synthesis and polymer science. Transition metal mediated metathesis was already described by Chauvin et al. in 1971.[6] In his publication he suggested a mechanism where a [2+2] cycloaddition forms a metallacyclobutane intermediate which then undergoes a cycloreversion to form the final product.

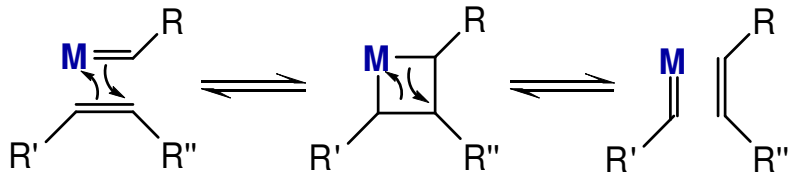

Scheme 2: Chauvin's mechanism of olefin metathesis

Together with Robert H. Grubbs and Richard R. Schrock, Yves Chauvin received the Nobel Prize for chemistry in 2005 for "the development of the metathesis method in organic synthesis". Two of the most important applications for metathesis in organic synthesis are **R**ing **O**pening **M**etathesis **P**olymerization and **R**ing **C**losing **M**etathesis. The according reaction mechanisms are depicted below.

[6] Hèrisson, J. L.; Chauvin, Y. *Makromol. Chem.*, **1971**, *141*, 161-176.

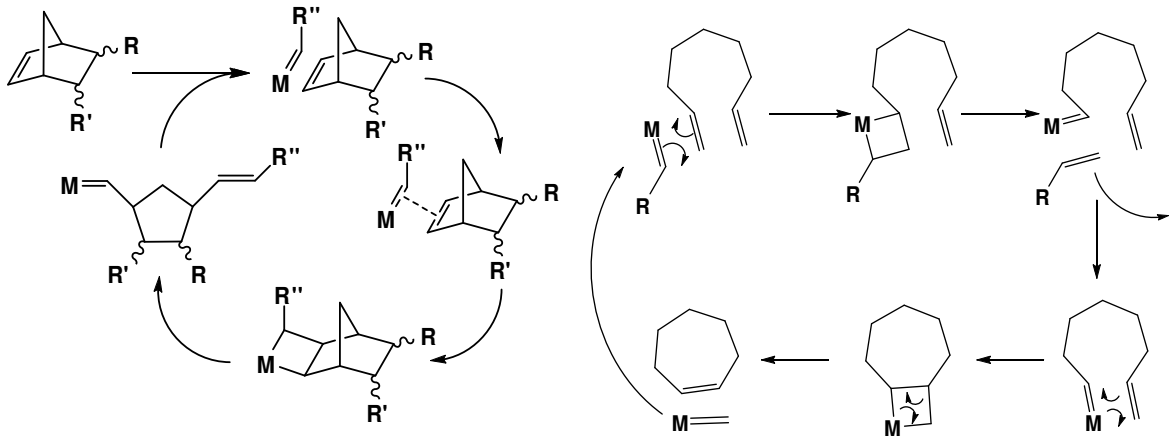

Scheme 3: Reaction mechanisms of ROMP (left side) and RCM (right side)

2.2 Transition Metal Metathesis Initiators

Many transition metals have been investigated considering their applicability as organometallic initiators for olefin metathesis. The first successful single component complexes were realized using tungsten or molybdenum as the central atom, such as $[W(CH\text{-}Bu^t)(NAr)(OCCH_3(CF_3)_2)_2]$ (**1**) or $[Mo(CHCMe_2Ph)(N\text{-}2,6\text{-}i\text{-}Pr^i{}_2C_6H_3)\ (OCMe(CF_3)_2)_2]$ (**2**), two complexes that were introduced by Schrock.[7,8]

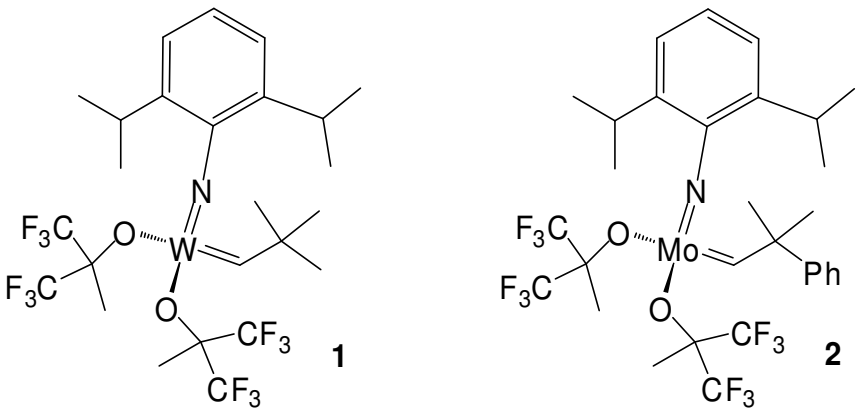

Fig. 2: Molybdenum and tungsten Metathesis catalysts of Schrock

Some determining drawbacks of these first metathesis catalysts were a high sensitivity towards oxygen and moisture and a rather low functional group

[7] Schrock, R. R. *Tetrahedron*, **1999**, *55*, 8141-8153.
[8] Schrock, R.R. *Acc. Chem. Res*. **1990**, *23*, 158.

tolerance, limiting their applicability severely. These problems were partly resolved by the introduction of ruthenium based carbene complexes. The breakthrough for metathesis chemistry came with the work of Grubbs et al.[9] With $[(PCy_3)_2(Cl)_2Ru=CHPh]$ (**3**), the so called "1st generation" of ruthenium based metathesis catalysts was born. As for Ring Opening Metathesis Polymerization, complex **3** shows high initiation rates because of easy dissociation of the phosphine from the ruthenium centre. At the same time, the phosphine's tendency to recoordinate rather than the approaching olefin causes low propagation rates, resulting in long reaction times. Further research on alternative ligands lead to the use of an N-heterocyclic carbene moiety.[10,11,12] When one phosphine ligand was replaced by such an NHC, a significant increase of reactivity due to the electronic influence on the ruthenium centre was observed.[13] The most prominent member of this so called "2nd generation", is "Super-Grubbs-catalyst" $[(H_2IMes)(PCy_3)(Cl)_2Ru=CHPh]$ (**4**).[14] As a strong σ - donor with very low π - acceptor capacity, the NHC ligand was thought to turn the phosphine more labile. Surprisingly, the opposite seems to be the case according to Ru – P bond lengths and the phosphine ligand is stabilized by the NHC ligand in *trans* position. [15,16] At the same time, recoordination of the phosphine is also hindered and the olefin can easier occupy the vacant coordination site. As a result, for complex **4**, initiates ROMP much slower than **3**, but enables faster propagation. However, this combination is not favourable for polymerizations, as it results in unwanted high polydispersity indices (PDI). Moreover, living polymerization and therefore the synthesis of block co-polymers is not provided by this type of initiator.

[9] Schwab, P.; Grubbs, R. H.; Ziller, *J. W. J. Am. Soc.*, **1996**, *118*, 100-110.
[10] Westkamp, T.; Schattenmann, W. C.; Spiegler, M.; Herrmann, W. A. *Angew. Chem.* **1998**, *110*, 2631-2633.
[11] Huang, J.; Stevens, E. D.; Nolan, S.P.; Peterson, J. L. *J. Am. Chem. Soc.* **1999**, *121*, 2674-2678.
[12] Scholl, M.; Ding, S.; Lee, C. W.; Grubbs, R. H. *Org. Lett.* **1999**, *1*, 953-956.
[13] Sanford, Melanie S.; Love, Jennifer A.; Grubbs, R. H. *J. Am. Chem. Soc.* **2001**, *123*, 6543-6554.
[14] Trnka, T. M.; Grubbs, R.H., *Acc. Chem. Res.* **2001**, *34*, 18-29.
[15] Scholl, M.; Trnka, T. M.; Morgan, J. P.; Grubbs, R. H. *Tetrahedron Lett.* **1999**, *40*, 2247-2250.
[16] Schwab, P.; Ziller, J. W.; Grubbs, R. H. *J. Am. Chem. Soc.* **1996**, *18*, 100-110.

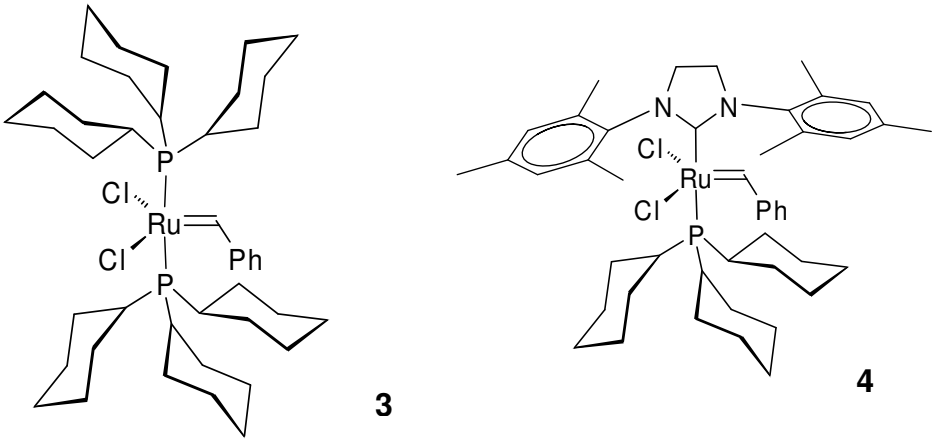

Fig. 3: Grubbs – catalysts: 1st generation (3) and 2nd generation (4)

Another innovative step concerning ruthenium based metathesis cataslysts was the introduction of phosphine free complexes. About contemporaneously, Slugovc and Grubbs found that pyridine or 3-bromopyridine are suitable ligands that, combined with H_2IMes – NHC provide perfect properties for a ROMP – initiator.[17,18] Interestingly, the resulting complexes exhibit two pyridine ligands, which replace only one phosphine ligand. This new design concept is called the "3rd generation" of Ru – catalysts".

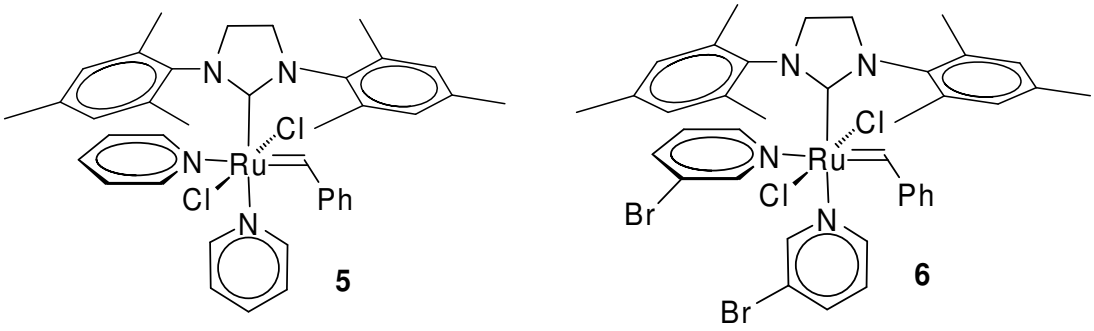

Fig. 4: 3rd generation catalysts: Slugovc's pyridine modified catalyst (**5**) and Grubbs' Br-pyridine analogue (**6**)

3rd generation catalysts perform greatly in ROM polymerizations. Initiation rates are immensely higher than in 2nd generation analogues, and propagation is very fast because pyridine hardly competes with the approaching monomer for a vacant coordination site at the ruthenium centre. As a result, obtained polymers show very low PDI values. Thanks to extremely short reaction times, living

[17] Love, J. A.; Morgan, J. P.; Trnka, T. M.; Grubbs, R. H. *Angew. Chem*. **2002**, *114*, 4207-4209.
[18] Slugovc, C.; Demel, S.; Stelzer, F. *Macromol. Rapid Commun*. **2003**, *24*, 435-439.

polymerisation and the synthesis of well defined, tailored block co-polymers is possible.[19]

2.3 Neolyst – Type Initiators

Both, the tremendous performance and the high price of the Grubbs – type – initiators provoked a lot of research on equipotent alternatives. Research on this carbene forming ligand system already started in 1982 by Selegue, and was then independently adopted by Dixneuf, Fürstner, Hill and Nolan.[20,21]

By now, a parallel system to Grubbs' 1st – 3rd generation system exists, where the benzylidene ligand is replaced by 3-phenylindenylidene. The German company Umicore AG is marketing indenylidene complexes labelled Neolyst M1 (**7**) and Neolyst **M2** (**8**) which correspond to **3** and **4**, respectively. In cooperation with our group, Neolyst **M3** (**9**), the 3rd generation analogue was developed. Its performance in controlled living ROM polymerization is comparable with that of **5**. Single crystal diffractometry showed that in contrast to complex **5**, only one pyridine moiety is coordinated.[22] This is contradicted by a publication of Nolan et al., where almost identical synthesis yielded a complex with two coordinated pyridine moieties.[23]

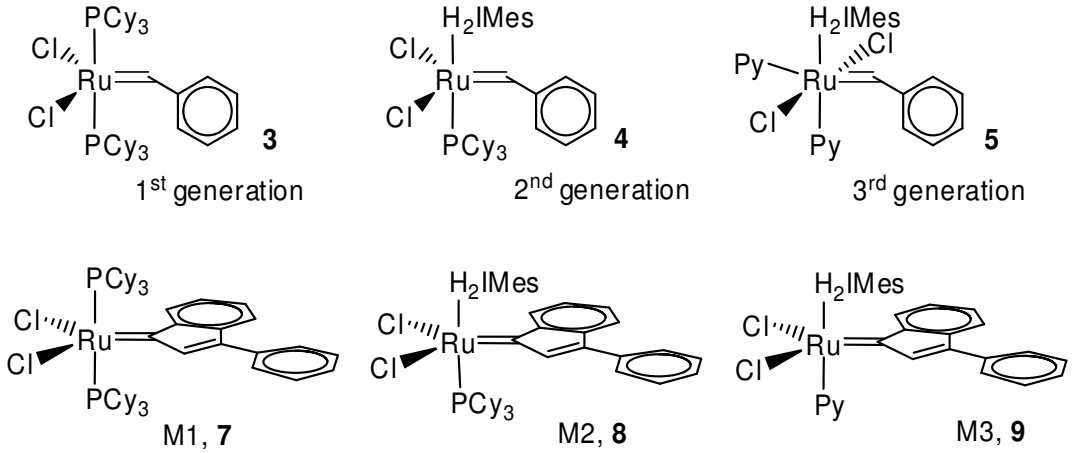

Scheme 4: Grubbs – type initiators and their corresponding Neolyst indenylidene analogues

[19] Slugovc, C.; Demel, S.; Stelzer, F. *Chem. Commun.* **2002**, 2572-2573.
[20] Compare: Boeda, F.; Clavoer, H.; Nolan, S. P. *Chem. Commun.*, **2008**, 2726-2740.
[21] Castarlenas, R.; Vovard, C.; Fischmeister, C.; Dixneuf, P.H. *J. Am. Chem. Soc*, **2006**, *128*, 4079-4089.
[22] Burtscher, D.; Lexer, C.; Mereiter, K.; Winde, R.; Karch, R.; Slugovc, C. . *Polym. Sci. Part A: Polym. Chem.* **2008**, *46*, 4630.-4635.
[23] Clavier, H.; Petersen, J. L.; Nolan, S.P. *J. Organomet. Chem*, *691*, **2006**, 5444-5447.

2.3.1 Transition Metal Complexes – 18 electron rule

A closer look at the coordination sphere of the ruthenium centre brings a better understanding about how metathesis can work. Valence shells of a transition metal can accommodate 18 electrons: 2 in each of the five d orbitals; 2 in each of the three p orbitals; and 2 in the s orbital. Combination of these atomic orbitals with ligand orbitals gives rise to molecular orbitals which are energy dispersive. The nine orbitals to be occupied first are metal-ligand bonding or non-bonding ones. The complete filling with electrons of these nine is the basis of the 18-electron rule.[24] Anti-bonding orbitals are energetically much higher and therefore normally not occupied. In practice, not all transition metal complexes fulfil the 18-electron rule. Depending on the position of the transition metal in the periodic table and the ligand's characteristics, also $14e^-$, $16e^-$, or even $>18e^-$ - complexes can be formed. There are three categories, summed up in the next table.

Table 1: Transition metals and their rough tendency to obey the 18 electron rule

18 electron rule	number of electrons	ligands	transition metal
1: don't obey	less, equal or more than 18 e^-	weak	↑ early
2: don't exceed	equal or less than 18 e^-	middle or strong	late
3: obey	18 e^-	strong	

Grubbs – or Neolyst – type complexes belong to the second category, with Ru standing in the 8th group of the periodic table and ligands in the middle or at the rear section of the spectrochemical series. The according MO diagram is depicted in the following.

[24] Mitchell, P. R.; Parish, J. The Eighteen-Electron Rule. *J. Chem. Educ.* **1969**, *46*, 811–814.

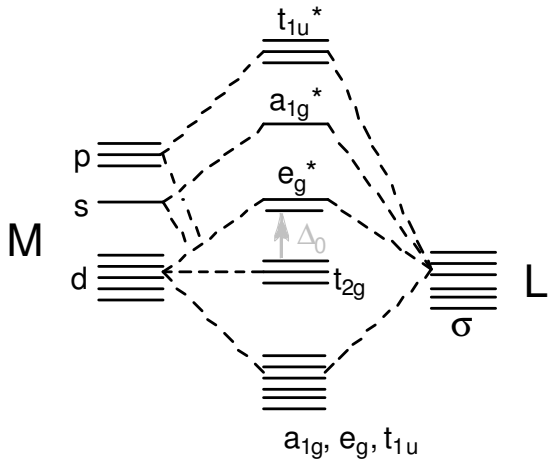

Fig. 5: MO – scheme of a transition metal – ligand bond.

The lowest six, binding orbitals are fully occupied. t_{2g} can be filled with 0 - 6 electrons. The anti – binding orbital e_g* is energetically too high to be occupied. This results in a possible number of 12 - 18 valence electrons.

As a consequence, there are different possibilities of how ruthenium mediated olefin metathesis can happen. The limiting cases are depicted and discussed in the following.

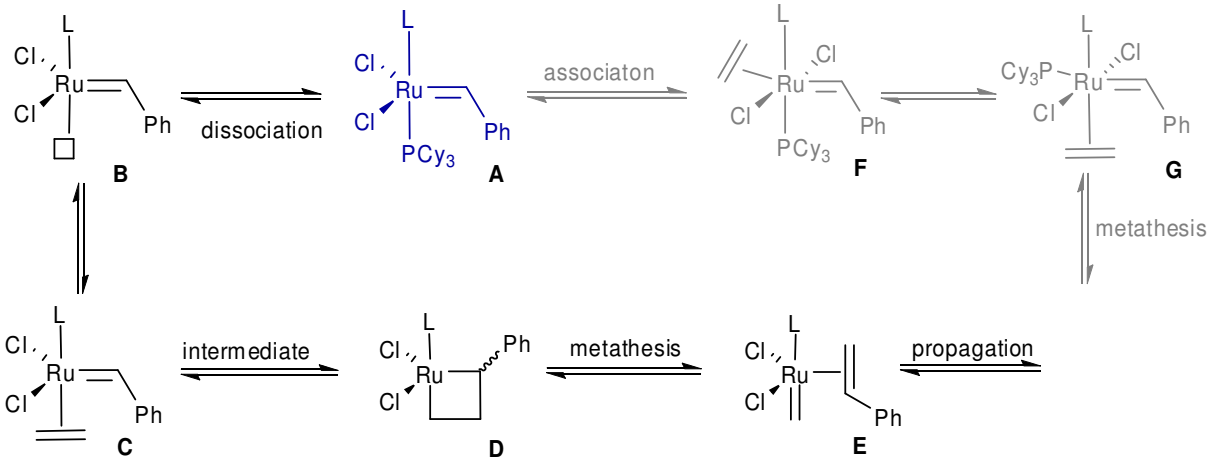

Scheme 5: Dissociative (black) and associative (grey) pathway for metathesis initiation of 1st generation (L = PCy3) and 2nd generation (L = NHC) initiators

In pathway A → F → G → (coloured in grey), an 18 e^- intermediate F is formed via association of an olefin. A configurational rearrangement towards G has to follow in order to bring the olefin in a favourable position for metathesis.
The second limiting case is a dissociative pathway, drawn in black. The phosphine ligand dissociates from the 16 e^- complex A to give a 14 e^- intermediate B. The gained free coordination site can be occupied by the olefin (C). Metalla cyclobutane D is formed before metathesis leads to a new 16 e^- complex E and the cycle can restart. The labile phosphine ligand can leave and enter the ruthenium's coordination sphere reversibly, establishing a possible equilibrium of G ↔ C. Thus, the two pathways are connected with each other. Kinetic studies on phosphine containing initiators like 3 and 4 found the dissociative pathway more likely to occur.[25,26] This theory is supported by the identification of the stable 14 e^- complex $[(H_2IMes)(OBu^t)_2Ru{=}CHPh]$.[27]

2.4 Tailoring the Applicability of Metathesis Initiators – Latent Initiators

Recent developments in organic electronics such as OLEDs (organic light emitting devices) or photovolataic devices have opened a wide field of research in many areas of physics and chemistry. In the polymer sector, suitable polymer designs for optimal charge transfer on the one hand and good processability on the other hand are needed. In some cases it would be desirable to polymerize only after processing (e.g. ink jet printing). Therefore, an initiator that can be mixed, stored and processed with the monomer without getting active is absolutely essential. After processing, polymerization should be fast and complete. The trigger for initiation can be heat or IR – irradiation. As described in the introduction, a chelating carbene ligand at the ruthenium centre was considered to be the most promising approach.

[25] Dias, E. L.; Nguyen, T., S., Grubbs, R. H. *J. Am. Chem. Soc*. **1997**, *119*, 3887-3897.
[26] Sanford, M. S.; Ullmann, M., Grubbs, R. H. *J. Am. Chem. Soc*. **2001**, *123*, 6543-6554.
[27] Sanford, M. S.; Henling, L. M.; Day, M. W.; Grubbs, R. H. *Angew. Chem. Int. Ed*. **2000**, *39*, 3451.

2.4.1 Oxygen Donor Ligands

In 1999 Hoveyda et al published the synthesis and characterization of a ruthenium complex derived from Grubbs' 1st generation catalyst 3, bearing a chelating benzylidene ether ligand (10).[28] The complex was found to be a potent catalyst for RCM under ambient atmosphere. Moreover, the "Hoveyda – catalyst" can be recycled by silica gel chromatography without forfeiting its activity.

Later, the phosphine free so-called "Super – Hoveyda" catalyst (**11**) was obtained by modifying the 2nd generation type by a metathesis reaction.[29]

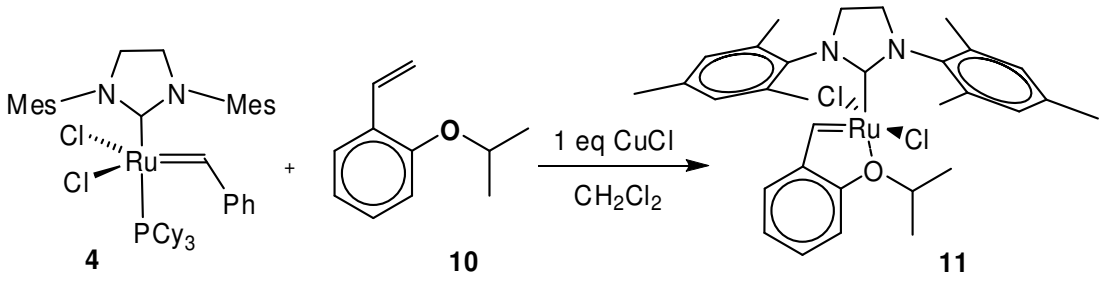

Scheme 6: Synthesis of "Super – Hoveyda" catalyst (**11**) using Grubbs' 2nd generation catalyst and isopropoxy styrenyl ether (**10**).

Even if **11** represents a design motive for latent initiators, the chelating bond is too weak to disable metathesis at room temperature. Fürstner and Slugovc investigated the according ester functionalized ligand, where the carbonyl oxygen coordinates to the metal centre to form a six – membered ring.[30,31] Further derivatives were synthesized in our group. In according temperature dependent ROMP experiments with these ester derivatives (depicted in the following figure), polymerization was not prevented at room temperature, though.

[28]Kingsbury, J.S.; Hatrriy, J.P.A., Hoveyda, A.H., *J. Am. Chem. Soc.*, **1999**, *121*, 791-799.
[29] Garber, S. B.; Kingsbury, J.S.; Gray, B. L.; Hoveyda, A.H. *J. Am. Chem. Soc.*, **2000**, *122*, 8168-8179.
[30] Fürstner, A.; Thiel, O.R.; Lehmann, C.W., *Organometallics*, **2002**, *21*, 331-335.
[31] Slugovc, C.; Perner, B.; Stelzer, F.; Mereiter, K. *Organometallics* **2004**, *23*, 3622-3626.

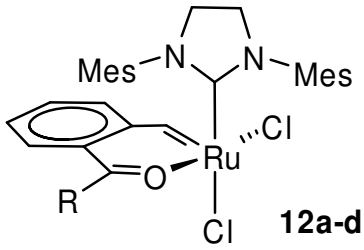

Fig. 6: Chelating ester derivatives

2.4.2 Nitrogen Donor Ligands

Van der Schaaf et al. described ruthenium complexes bearing chelating 2-pyridylethanyl – carbene igands.[32] Nitrogen, being a stronger electron donor should increase the chelate's bond strength. Indeed, with enamine ligands like phenyl(2-vinylbenzylidene)amine (complex **13**) or benzylidene-(2-vinylphenyl)amine (complex 14) significant elevated switching temperatures for ROMP (55 °C and 48 °C, resp.) were achieved.[33]

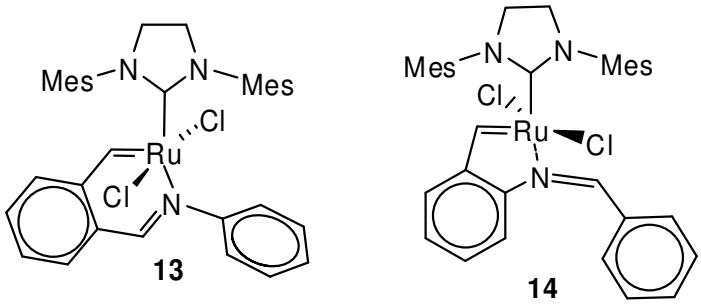

Fig. 7: Ruthenium complexes bearing nitrogen donors as chelating ligands

A study concerning the influence of the chelate's ring size in nitrogen donor ligands showed that 5 – membered rings are less stable than six – membered rings, which is reflected in the switching temperatures of the initiators.[34]

[32] Van der SChaaf, P. A.; Kolly, R.; Kirner, H.-J.; Rime, F.; Mühlebach, A.; Hafner, A. J. *J. Organomet. Chem*. **2000**, *606*, 65-74.
[33] Slugovc, C.; Burtscher, D.; Stelzer, F.; Mereiter, K. *Organometallics*, **2005**, *24*, 2255-2258.
[34] Slugovc, C.; Burtscher, D.; Stelzer, F.; Mereiter, K. *Organometallics*, **2005**, *24*, 2255-2258.

2.4.3 Phosphorus Donor Ligands

Diphenyl-(1-phenylvinyl)-phosphine was used to achieve complex **15**. Switching temperature (42 °C) was determined with DSC experiments.[35]

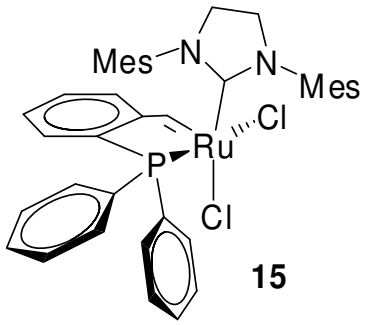

15

Scheme 7: Ruthenium catalyst bearing a chelating ligand with phosphorus as donating species

2.4.4 Sulphur Donor Ligands

Lemcoff et al. published a series of latent ruthenium olefin metathesis catalysts with a switching temperature of up to 80°C. It's derived from Grubbs' 2nd generation catalyst which undergoes metathesis with different styrene isopropyl thioether derivatives to form **16a-e**.[36]

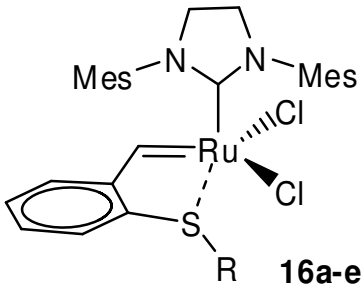

16a-e

a) R = Bu^t
b) R = Ph
c) R = Pr^i
d) R = Et
e) R = Me

Fig. 8: Sulphur as chelating species in a thermally switchable initiator

The influence of bulkiness and electronic constitution of R on the chelate's strength and therefore the initiator's activity was investigated by comparative RCM experiments with DEDAM. In the process, temperature was raised from 25 to 100 °C stepwise. Results are depicted in the following picture.

[35] Diploma Thesis, Bernhard Perner, Graz 2004.
[36] Kost, T.; Sigalov, M.; Goldberg, I.; Ben-Asuly, A.; Lemcoff, N. G. *J. Organomet. Chem.*, **2008**, *693*, 2200-2203.

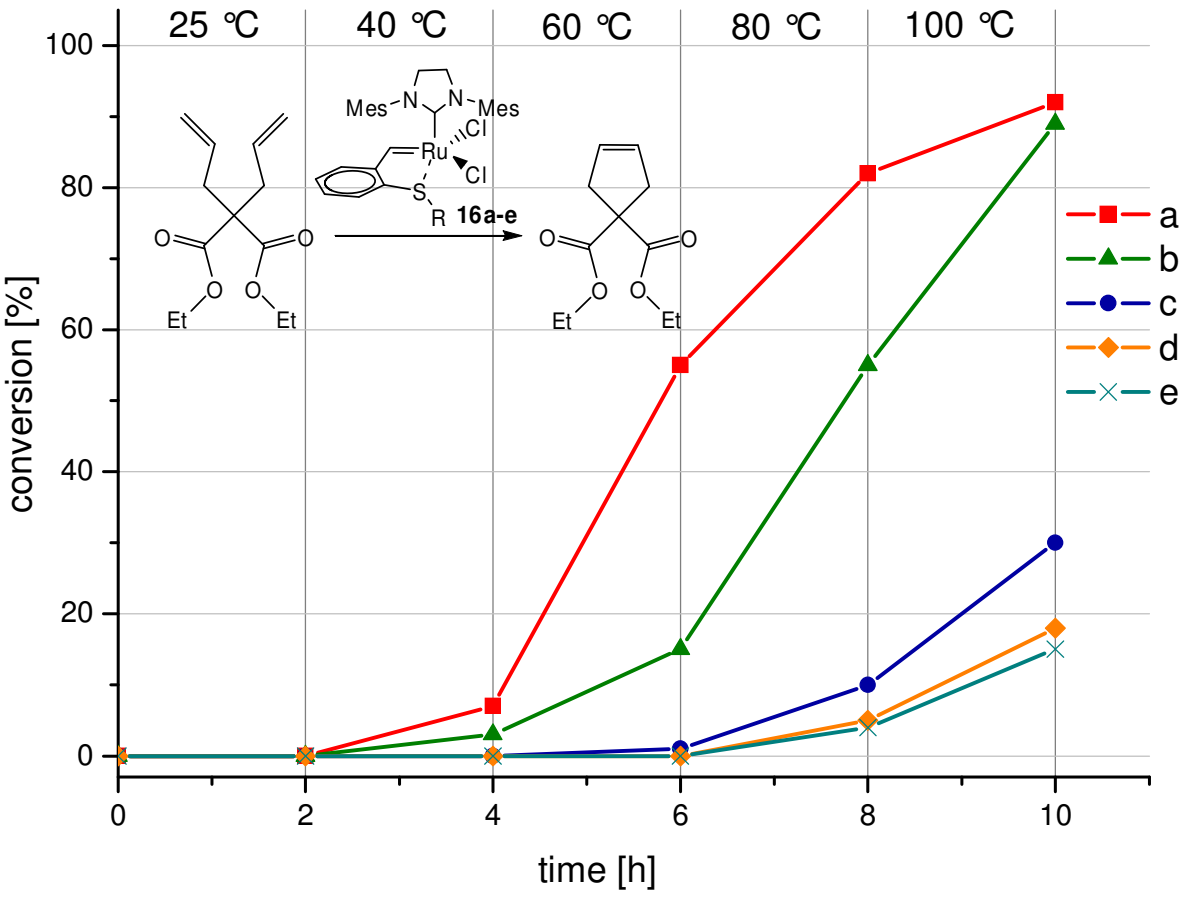

Fig. 9: RCM reaction with DEDAM and **16a-e**. Temperatures were kept constant for two hours each.

For **16a**, the sterical demanding *tert*-butyl residue is responsible for the high activity. However, it seems that 16a decomposes at higher temperatures. In contrast, the phenyl group in 16b withdraws electron density from the sulphur's lone pairs and weakens the chelate that way. No decomposition can be noted at 100 °C.

With complex **16c** (switching temperature = 80 °C) conversion was only 30 % at the end of the experiment. No degradation can be noted at 100 °C. **16c** can be turned on and off totally reversibly, as proved in RCM experiments with an alternating temperature program.[37] Both, **16d** and **16e** bear very small substituents that lead to a strong S – Ru bond, resulting in a high switching temperature and low conversion.

[37] Ben-Asuly, A.; Tzur, E.; Diesendruck, C. E.; Sigalov, M.; Goldberg, I.; Lemcoff, N. G. *Organometallics* **2008**, *27*, 811-813.

2.5 Summary

Ruthenium in transition metal catalysts emerged as the most promising candidate for olefin metathesis reactions. Significant advantages are given by easier handling and unrivalled high functional group tolerance. The following table gives an overview comparing early and late transition metals in their reactivity towards different substrates.

Table 2: Functional group tolerance of titanum, tungsten, molybdenum and ruthenium

Ti	W	Mo	Ru
Acids	Acids	Acids	Olefins
Alcohols, Water	Alcohols, Water	Alcohols, Water	Acids
Aldehydes	Aldehydes	Aldehydes	Alcohols, Water
Ketones	Ketones	Olefins	Aldehydes
Esters, Amides	Olefins	Ketones	Ketones
Olefins	Esters, Amides	Esters, Amides	Esters, Amides

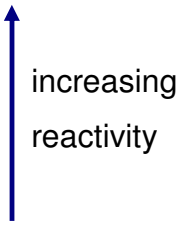

Thermally switchable initiators are of great interest due to the latest developments in organic electronics. The concept of chelating carbene ligands already yielded some promising results. Impact factors like the chelating species and the chelate's ring size are to be further investigated.

3 RESULTS AND DISCUSSION

The aim of this work was to synthesize new types of Ruthenium initiators bearing chelating carbene ligands. Many different ligands of this type have been investigated during the last decade, including an functionalities such as ethers,[38] esters,[39] phosphines,[40] enamines[41] or sulphides.[42]

Within this work, all synthesized ligands bear an amide functionality as the chelating moiety in *ortho* position to the vinyl group. The amide establishes two possibilities for the chelation towards the ruthenium centre. Chelation via the carbonyl oxygen as well as the amide nitrogen would lead to a six-membered ring which is likely to be formed due to its low ring strain.

3.1 Ligands

In most cases, the amide ligands were prepared through a two step reaction starting from 2-bromobenzoylchloride. In the first step, the amidation was carried out in CH_2Cl_2 using the corresponding amine and pyridine as base. The reaction was started at 0°C and brought to room temperature over night; its progress was monitored via TLC. After washing with HCl (10%) and saturated $NaHCO_3$, solvent was removed and if necessary, the crude product was purified by column chromatography. Yields ranged from 51 – 76%. The reaction scheme is shown below.

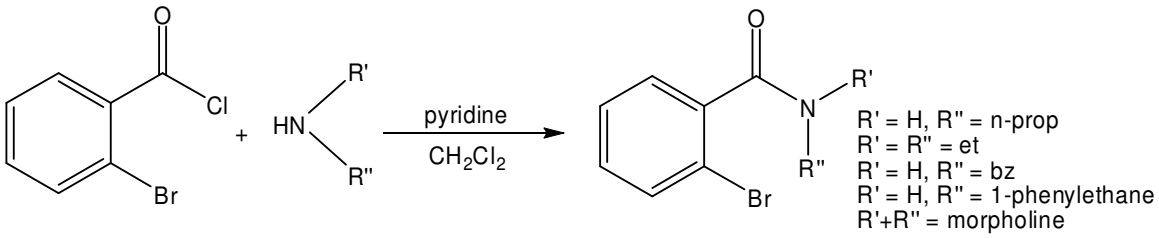

Scheme 8: Amidation

[38] Kingsbury, J.S.; Hatrriy, J.P.A., Hoveyda, A.H., *J. Am. Chem. Soc.*, **1999**, *121*, 791.
[39] Slugovc, C.; Perner, B.; Stelzer, F.; Mereiter, K. *Organometallics* **2004**, *23*, 3622.
[40] Diploma Thesis, Perner Bernhard, Graz, 2004.
[41]. Slugovc C.; Burtscher, D.; Mereiter, K.; Stelzer, F., *Organometallics* **2005**, *24*, 2255.
[42] Ben-Asuly, A.; Tzur, E.; Diesendruck, C.E.; Sigalov, M.; Goldberg, I.; Lemcoff, N.G., *Organometallics* **2008**, *27*, 811-813.

In the second step, two different approaches for the vinylation of the phenylbromide derivatives were tested and compared. With Suzuki cross-coupling reactions, all secondary amides furnished their corresponding vinyl derivative in good yields. In this reaction, the bromide was allowed to react with a vinyl boronic anhydride pyridine complex in presence of K_2CO_3 and catalytic amounts of $Pd(PPh_3)_4$ (2 mol%) in a solvent mixture of DME and water.

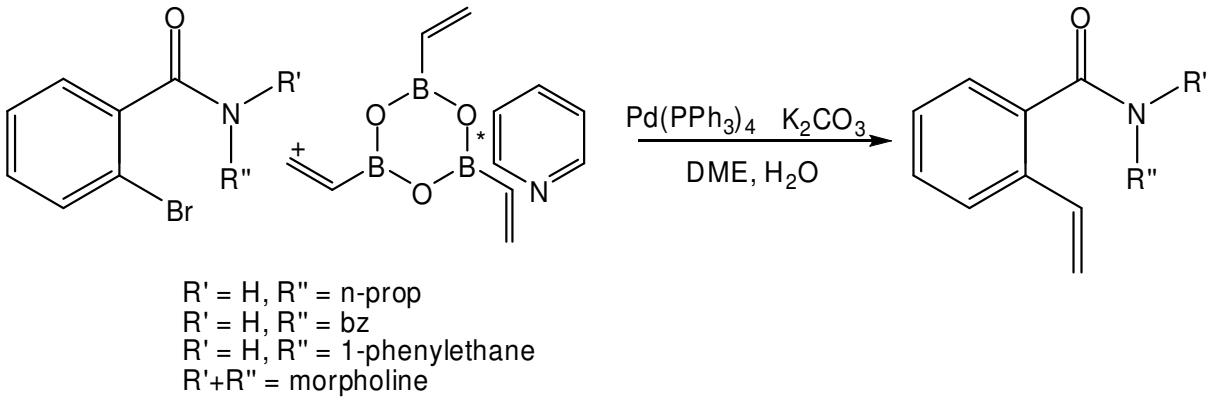

R' = H, R" = n-prop
R' = H, R" = bz
R' = H, R" = 1-phenylethane
R'+R" = morpholine

Scheme 9: Vinylation via Suzuki cross coupling

It turned out that when a tertiary amide had been used, the Suzuki coupling did not work out too good as a conversion of only 35% was obtained. Therefore, an alternative reaction method for the formation of *ortho* substituted vinylbenzamides was searched and found. Alacid et al. described a palladium catalyzed Hiyama reaction of vinyltrialkoxysilanes and *para* substituted arylbromides performed in basic aqueous solution using microwave irradiation.[43] The reaction conditions were adapted in order to get tertiary *o* – vinyl-benzamides: An aqueous solution of NaOH (0.5 M) was put into a microwave Teflon® liner and loaded with the accordant bromide, trimethoxyvinylsilane, TBAB (Tetrabutylaminobromide) as transferring reagent and catalytic amounts of $Pd(OAC)_2$ (10 mol%) under vigorous stirring. The reaction mixture was subjected to a temperature controlled microwave program which resulted, in the desired vinyl derivative in acceptable purity and yields, after filtration of the catalyst's decomposition products and extraction of organic components into Et_2O.

[43] Alacid, E.; Nájera, C. *J. Org. Chem.* **2008**, *73*, 2315-2322.

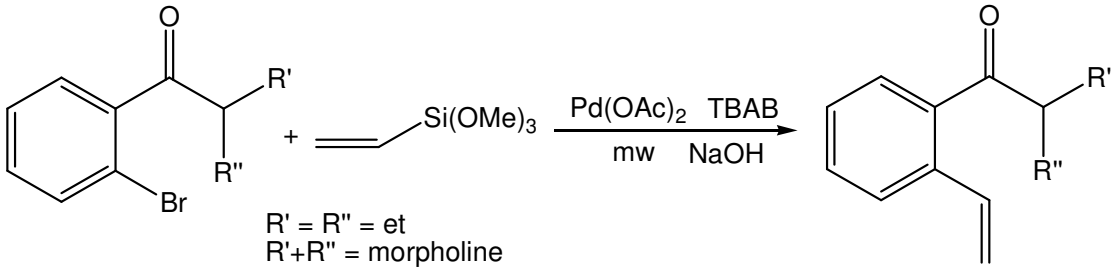

Scheme 10: Typical procedure for a Hiyama reaction

Another type of amide ligand was synthesized via a Suzuki coupling starting from an aniline derivative to get N-(2-vinylphenyl)amide derivatives. The very same reaction has been done and published by Cottineaou et al. wherefrom reaction conditions were adopted.[44] Yield was 54% after column chromatography.

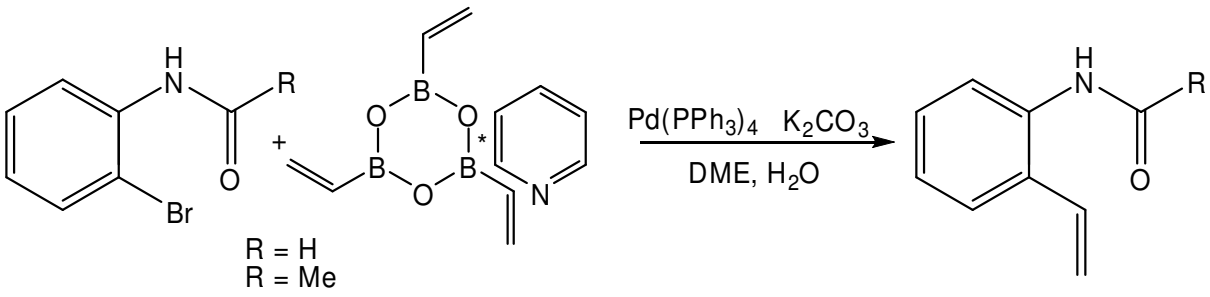

Scheme 11: Vinylation of an anilide with Suzuki coupling

The success of a vinylation can be easily controlled by ^{1}H-NMR spectroscopy, due to the characteristic vinyl signals. An example is shown in the following scheme.

[44] Cottineau, B.; Kessler, A.; O'Shea, D.F.; *Org. Synth.*, **2006**, *83*, 45-48.

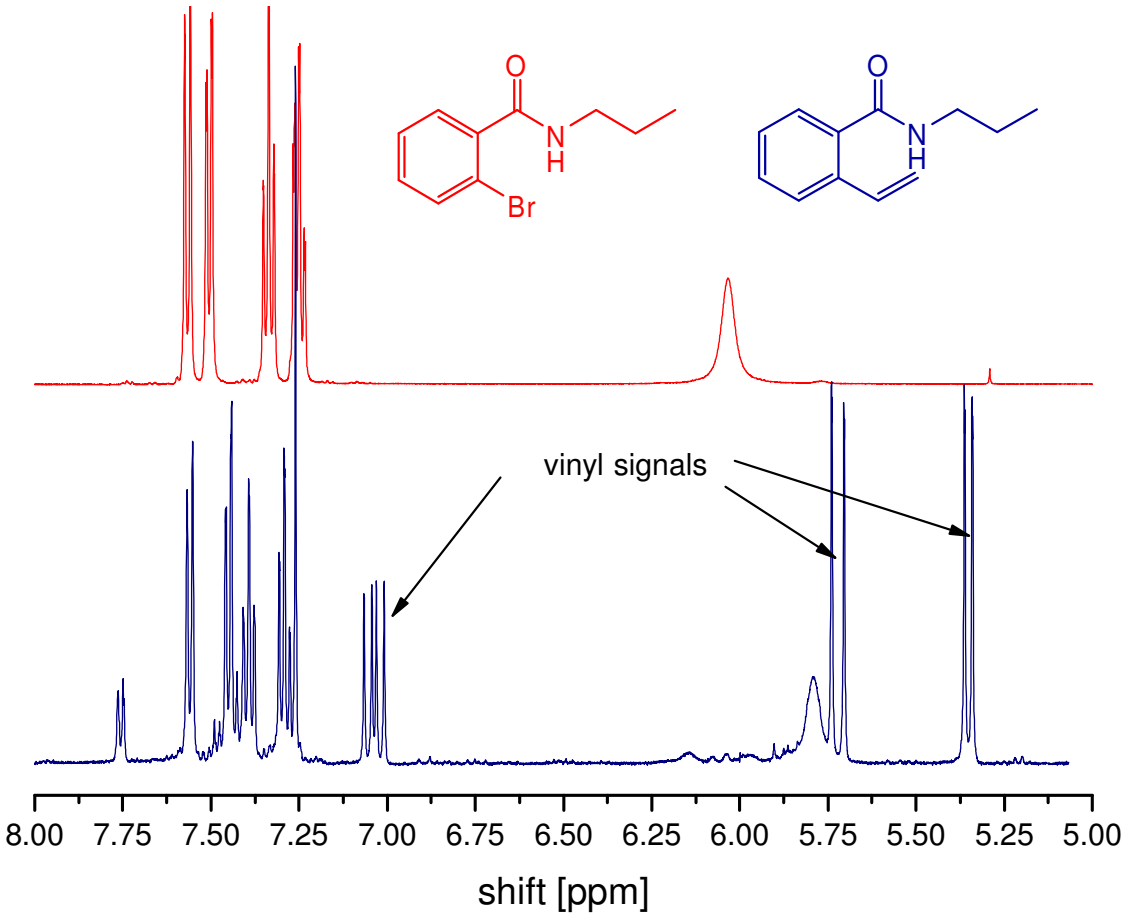

Fig. 10: Comparison of 1H-NMR spectra of 2-Bromo-N-propylbenzamide (above) and 2-vinyl-N-propylbenzamide

Concluding the synthesis of amide substituted carbene precursors for ruthenium based olefin metathesis initiators it can be said that substituted secondary vinylbenzamides are easily obtained by using Suzuki cross coupling. The Hiyama reaction increased yields for tertiary amide derivatives drastically, but still, results are not overwhelming. For an overview, obtained yields are summarized in the following table.

Table 3: Ligand overview

Vinyl derivative	Nr	Yield	Coupling
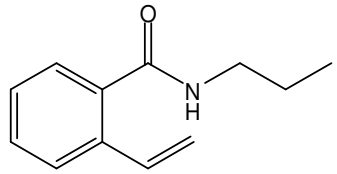	**17b**	84%	Suzuki
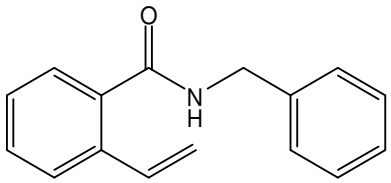	**18b**	76%	Suzuki
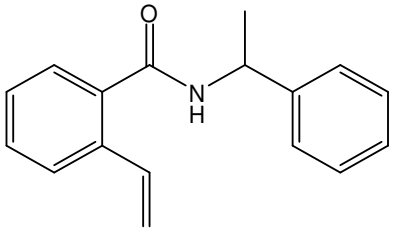	**19b**	58%	Suzuki
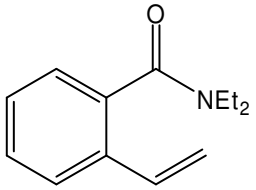	**20b**	60%	Hiyama
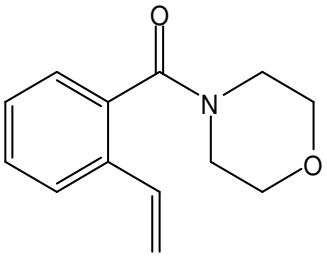	**21b**	70%	Hiyama
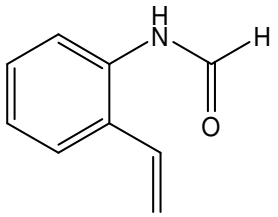	**22**	45%	Suzuki*
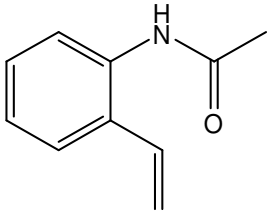	**23**	53%	Suzuki*

*Hiyama coupling was not performed

3.2 Complexes

The synthesized ligands were subsequently used to perform a carbene exchange reaction with a commercially available Ru(II) initiator. Thus, a new type of initiator bearing a chelating amide-based ligand at its active site should be created. A very common starting material for such reactions is Grubbs' 2nd generation catalyst that is normally used together with CuCl in order to capture the released phosphine ligand.[45]

However, for this work an alternative complex, Neolyst **M3** (**9**) which is similar to pyridine-modified Grubbs' 2nd-generation-catalyst, was used for the synthesis of almost all complexes. This much cheaper ruthenium compound has been recently developed by the German company UMICORE in collaboration with TU Graz. Its applicability for such reactions was already proven in the synthesis of ruthenium complexes bearing ester based ligands.[46] The main difference to the Grubbs type catalysts lies in an indenylidene ligand which replaces the benzylidene in related Grubbs – type complexes (see scheme below).

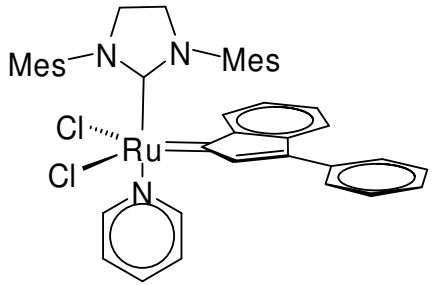

Fig. 11: Neolyst **M3** (**9**)

For the synthesis of the desired Ruthenium complexes several reaction conditions have been tested. The best results were obtained when the reaction mixture was allowed to stir overnight at room temperature using $CHCl_3$ as a solvent. A typical reaction is depicted below.

[45] Garber, S. B.; Kingsbury, J. S.; Gray, B. L.; Hoveyda, A. H. *J. Am. Chem. Soc.* **2000**, *122*, 8168-8179.
[46] Diploma Thesis, Bernhard Perner, Graz, 2004.

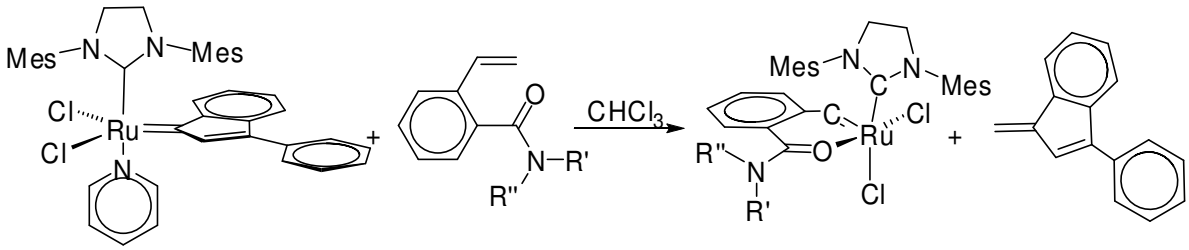

Scheme 12: Typical procedure for the formation of a new Ruthenium complex

Workup was mainly done by subsequent column chromatography using a mixture of cyclohexane and acetylacetate for elution of residual ligand and compensated methylene-3-phenylindene, and a CH_2Cl_2 : MeOH mixture for elution of the complex. In some cases precipitation upon Et_2O or *n*-pentane preceded and facilitated or even made chromatography needless.

In case of ligands **17**, **18**, **20** and **21** a successful carbene exchange could be observed by monitoring the reaction using ^{1}H-NMR spectroscopy: Due to the quaternary carbene carbon atom next to the Ruthenium centre in Neolyst **M3**, the characteristic carbene signal which was observed between 15 and 20 ppm clearly points out a replacement of the indenylidene ligand by the vinyl component. Unfortunately, in most cases two or even three carbene signals were observed indicating the formation of several species. Some investigations have been made on this matter which will be described in the next chapter.
Another conclusive evidence indicating success of the carbene exchange reaction is the isolation of the leaving group methylene-3-phenylindene (**28**) by means of chromatography. The according NMR spectrum is described in the chapter “Experimental Part”.
In the following, some discussion guiding through the range of performed experiments and the resulting conclusions is done by means of the model compound of this work, which is shown below. This complex was comparatively easily obtained and therefore used for most of the tests.

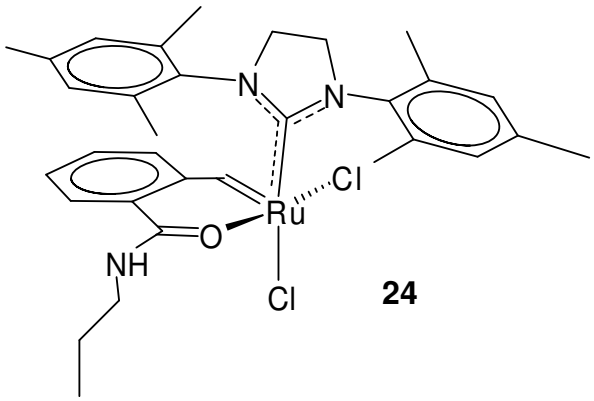

24

Fig. 12: Structure of **24**.

3.3 NMR-Spectroscopy

Even after purification on silica columns, ^{1}H-NMR spectra of the synthesized Ruthenium complexes turned out to be rather complicated as many inexplicit signals could not be assigned to the desired product. In order to get a rough overview about the obtained NMR spectra, analysis was divided into three parts.

3.3.1 Carbene region

As already mentioned before, success of the carbene exchange can be detected via characteristic carbene signals in the extreme low field region of the spectrum. Kinetic experiments, in which a spectrum was recorded every five minutes for the period of two and half hours showed the quick formation of a carbene peak at 19.2 ppm which was then slowly replaced by a signal at 17.6 ppm. However, complete conversion into the latter compound was not achieved In accordance with e.g. Grela, Slugovc, Fürstner, or Lemcoff, a plausible explanation for these two species is an isomerization from the kinetic *trans* chloro product to the thermodynamic *cis* chloro product. [47,48] Sometimes however, an additional, rather weak signal occurred at 18.7ppm indicating an even more complex system.

[47] Ben-Asuly, A.; Tzur, E.; Diesendruck, C.E.; Sigalov, M.; Goldberg, I.; Lemcoff, N.G. *Organometallics,* **2008**, *27*, 811-813.
[48] Barbasiewicz, M.; Szadkowska, A.; Bujok, R.; Grela, K., *Organometallics*, **2006**, *25*, 3599-3604.

3.3.2 Aromatic region

Typical ^{1}H-NMR spectra displayed more aromatic signals than expected. Some could be assigned to not-separated free amide ligand, some of them remained unassigned though. Whereas aromatic signals of the coordinated amide ligand could be identified in most cases, unequivocal assignment of mesityl signals revealed some difficulties. Additionally, some more signals were observed, which were not assigned at first sight. In the following exemplary spectrum only one carbene peak remained after column chromatography. Its intensity was determined to be “one” in order to quantify the other signals. While two of the four mesityl protons were observed as a broad singulet with an intensity of 2H at 6.15 ppm, the other two might be responsible for the broad singulets (1H each) at 8.85 and 8.31 ppm. The aromatic protons of the amide bearing ligand were assigned to the peaks at 7.75 ppm (t), 7.56 ppm (t) and 7.40 ppm (d, $^{3}J_{HH}$ = 7.5 Hz). One duplet was not observed and is presumably submersed under the solvent peak.

Remaining signals at 8.45 ppm (d, $^{3}J_{HH}$ = 5.2 Hz), 7.89 ppm (t) and 7.22 ppm (t) were tentatively assigned to a weakly coordinated pyridine molecule.

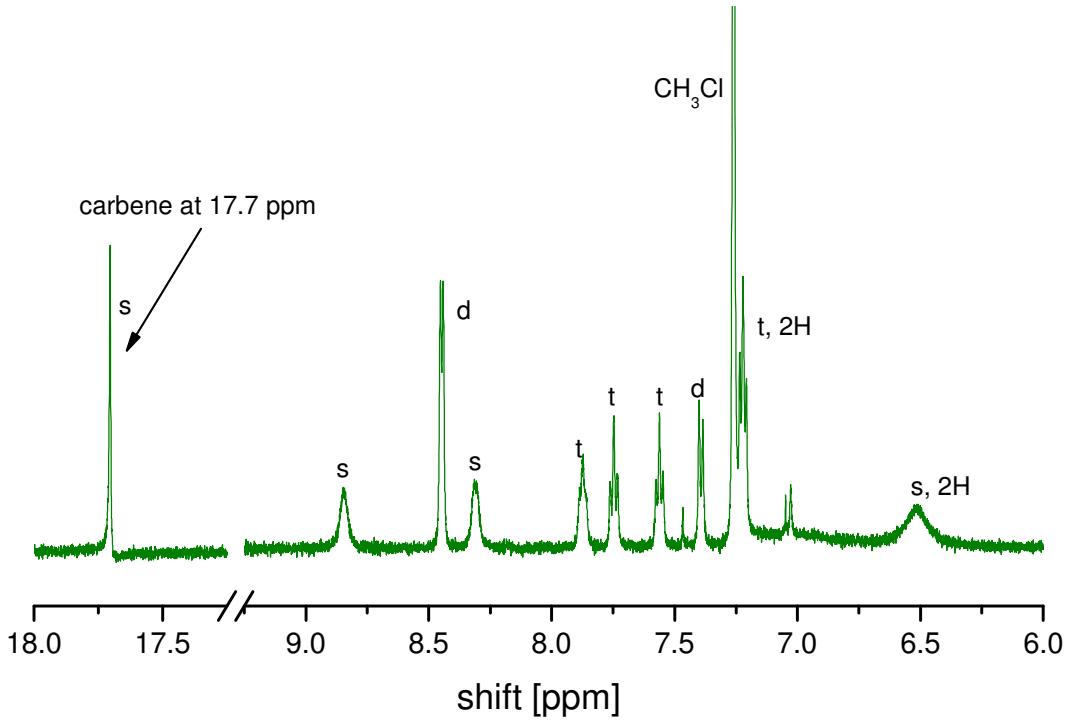

Fig. 13: Detail of 1H-NMR spectrum of complex **24** containing the carbene peak and the aromatic range. The spectrum recorded after column chromatography. An oversupply of aromatic signals is detected.

3.3.3 Aliphatic region

Expected peaks would rise signals from hydrogen atoms of the methyl groups and the saturated imidazole of the NHC ligand on the one hand and on the other hand the aliphatic part of the amide ligand.

Methyl groups of the NHC ligand could not be assigned definitely as they gave broad, inexplicit peaks that were often overlaid by signals not appendant on the complex. Presumably, the signals of methyl groups broadened because the measurement was carried out close to the coalescence temperature. In order to facilitate interpretation of the NMR spectrum, some measurements at elevated temperatures (20, 30, 40, 50 °C, $CDCl_3$ as solvent) were carried out.[49] Unfortunately even 50 °C was not enough to see a clear difference in the spectra. Lemcoff et al. reported similar findings, where a full coalescence of the methyl signals of a comparable complex was only observed at 145 °C.

3.4 MALDI-TOF MS

With this information at our disposal, MALDI-TOF (matrix assisted laser deposition ionisation – time of flight) mass spectrometry at high resolution was performed[50] with the aim to determine the stoichiometry of the complex. For this purpose, a clean product obtained from ether diffusion was used. It turned out that the crystal-like solid was hardly soluble in any solvent. Nevertheless, enough of the product was dissolved to perform the measurements.

[49] Ben-Asuly, A.; Tzur, E.; Diesendruck, C. E.; Sigalov, M.; Goldberg, I.; Lemcoff, N. G. *Oraganometallics*, **2008**, *27*, 811-813.

[50] MALDI-TOF investigations performed by K. Bartl and R. Saf

Table 4: Expected and obtained results of MALDI-TOF MS

structure of **24**	**24** with pyridine	found fragment
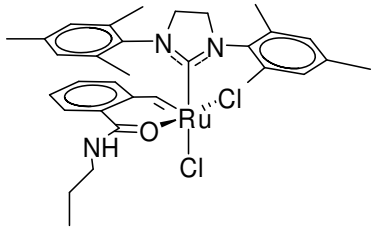	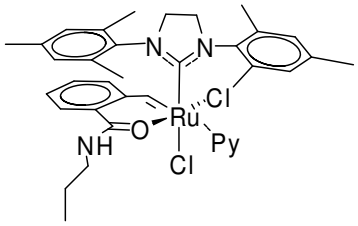	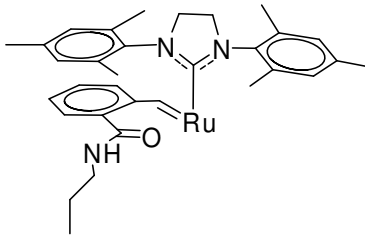
653.15 g/mol	731.19 g/mol	583.21 g/mol

It can be assumed that the ionization process leads to dissociation of the chloro ligands. In the following, a theoretically calculated isotope pattern for the resulting complex fragment, consisting of the ruthenium, the NHC – and the amide ligand, is depicted together with the experimentally obtained spectrum.

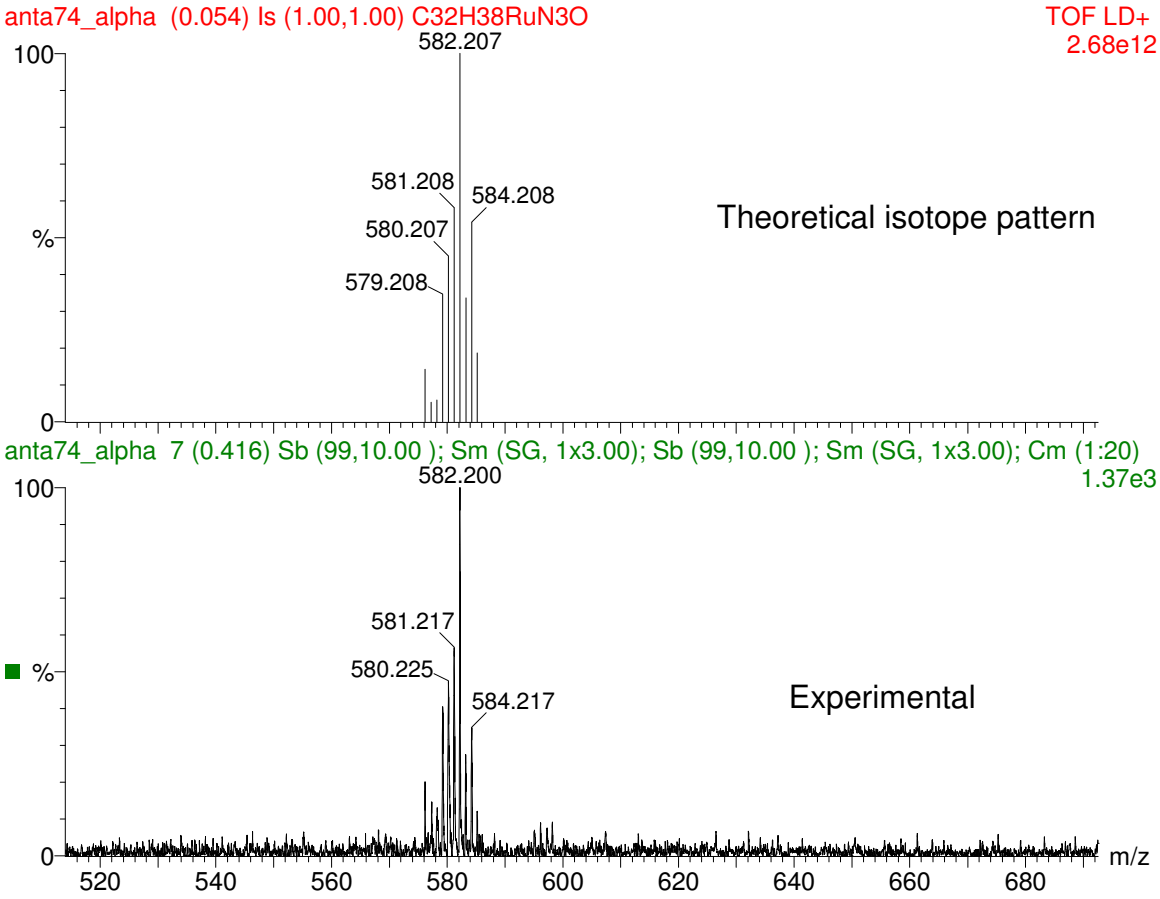

Fig. 14: MALDI-TOF spectrum of **24**.

The obtained spectrum is identical to the calculated isotope pattern of the complex fragment. No evidence for a coordinated pyridine was retrieved.

3.5 Crystal structure

In order to get pure substances and more information about feasible configurations, crystallization by ether diffusion was performed with some of the obtained ruthenium complexes, in particular with **24**. After some unsuccessful tries under air, the whole procedure was carried out under Argon atmosphere in a Schlenk flask, in order to prevent decomposition by oxygen interference. In case of 24, suitable crystals were obtained after several days, which were then subjected to X-ray diffractometry (performed by Prof. Kurt Mereiter, Vienna, University of Technology).

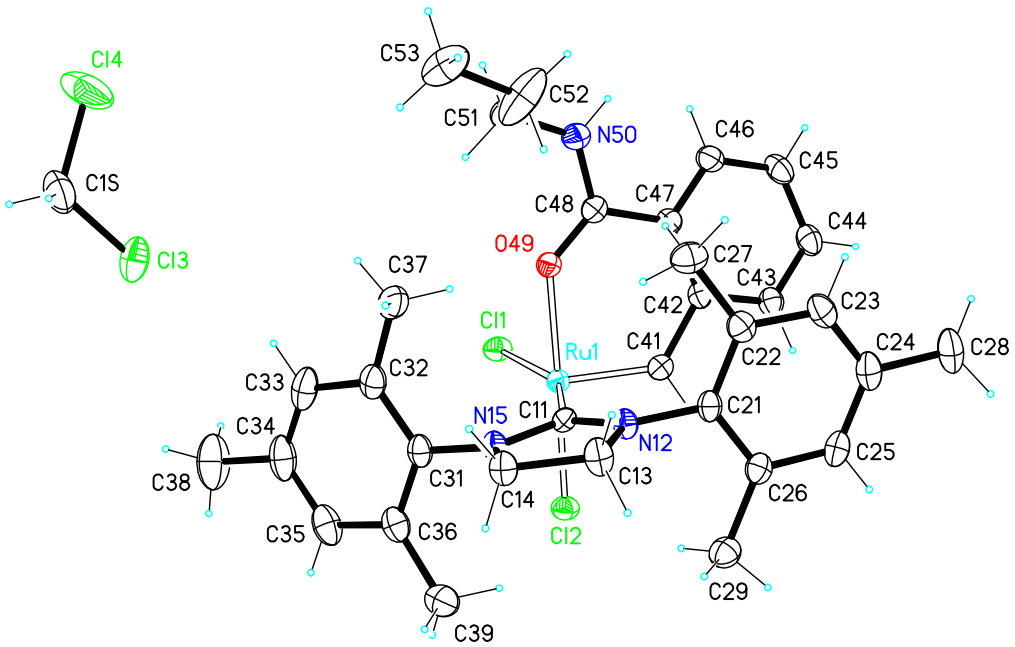

Fig. 15: Crystal structure of **24**, measured on Bruker “Kappa APEX-2” diffractometer.

Chloro ligands are in *cis* position to each other. The chelation of the amide ligand takes place via the carbonyl oxygen like in an ester and not via the nitrogen. The N-H forms a hydrogen bond to a chlorine ligand of a neighboured complex. Dichloromethane is integrated loosely into the crystal lattice. No evidence for a pyridine coordination was obtained.

Selected bond lengths and angles are summarized in the following table. To give a reference, comparison with a very similar ester derivative **25**, prepared by Bernhard Perner, is drawn.[51] Atom labels are adopted from the above crystal structure.

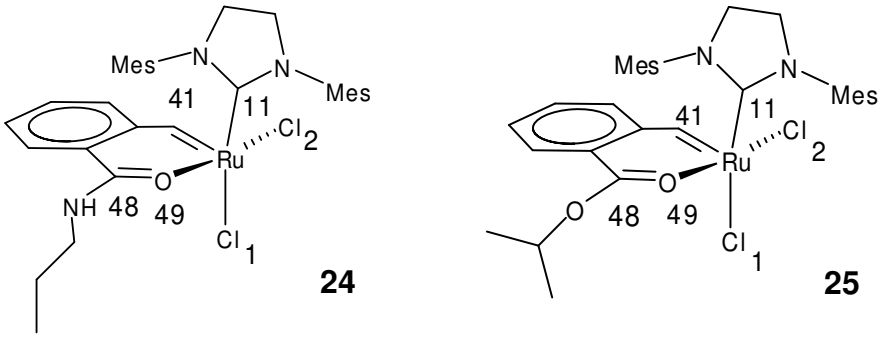

Fig. 16: Molecular structures of the obtained Ruthenium complex with an amide ligand (24) and a comparable ester derivative (**25**).

Table 5: Selected bond lengths of (24) and comparison with an ester derivative (**25**)

Bond	Bond length complex 24 [Å]	Bond length complex 25 [Å]	Difference [Å]
Ru – O49	2.080 (2)	2.093 (1)	-0.013
Ru – C41	1.815 (3)	1.815 (2)	0
Ru – C11	2.002 (2)	2.037 (2)	-0.035
Ru – Cl1	2.395 (1)	2.366 (1)	0.029
Ru – Cl2	2.369 (1)	2.362 (1)	0.007
C47 – C48	1.493 (4)	1.473 (3)	0.02
C48 – O49	1.253 (3)	1.236 (2)	0.017
C48 – X*	1.329 (3)	1.320 (2)	0.009
X* – C51	1.458 (4)	1.475 (3)	-0.017

*) X corresponds to N50 and the according oxygen in Amide and Ester, respectively

Only a few noteworthy differences can be claimed. In the amide, the Ru – NHC bond is somewhat shorter, whereas Ru – Cl1 and the carbonyl double bond are longer. However, the differences are in the one-digit percentage.

[51] Slugovc, C.; Perner, B.; Stelzer, F.; Mereiter, K. *Organometallics* **2004**, *23*, 3622-3626.

Table 6: Selected bond angles of 24 and comparison with an ester derivative (**25**)

Bond angle	Angle complex 24 [°]	Angle complex 25 [°]	Difference [°]
C41 – Ru – O49	89.19 (9)	89.90 (7)	-0.71
C41 – Ru – Cl1	108.03 (8)	103.40 (6)	4.63
C41 – Ru – Cl2	91.74 (8)	92.81 (6)	-1.07
C11 – Ru – O49	91.93 (9)	94.90 (6)	-2.97
C11 – Ru – Cl2	90.30 (7)	88.57 (5)	1.73
Cl1 – Ru – Cl2	88.52 (2)	89.85 (29	-1.33
O49 – C48 – C47	122.7 (2)	124.7 (2)	-2
O49 – C48 – X*	119.4 (2)	121.5 (2)	-2.1

*) X corresponds to N50 and the according oxygen in Amide and Ester, respectively

The most eye catching difference refer to Cl1 (line 2) and to the NHC ligand (line 4). All in all it can be said that the amide's nitrogen doesn't seem to have a large effect on the chelate's sterical characteristics.

3.6 Monitoring *cis* and *trans* configuration

The ester derivative described above had been synthesized by Fürstner et al before, but surprisingly appears to bear its chloro ligands in *trans* position.[52] The difference in synthesis lies in the starting material. Whereas Fürstner used Grubbs' 2nd generation catalyst with CuCl and toluene as solvent, Slugovc used the modified pyridine species and CH_2Cl_2 (compare figure below). It turned out, that when storing the *trans* product in solution, a rearrangement towards the *cis* configuration takes place. This was also observed for complexes bearing a quinoline based ligand by Karol Grela et al. in several complexes bearing chelating carbene ligands.[53]

[52] Fürstner, A.; Thiel, O.R.; Lehmann, C.W., *Organometallics*, **2002**, *21*, 331-335.
[53] Barbasiewicz, M.; Szadkowska, A.; Bujok, R.; Grela, K., *Organometallics*, **2006**, *25*, 3599-3604.

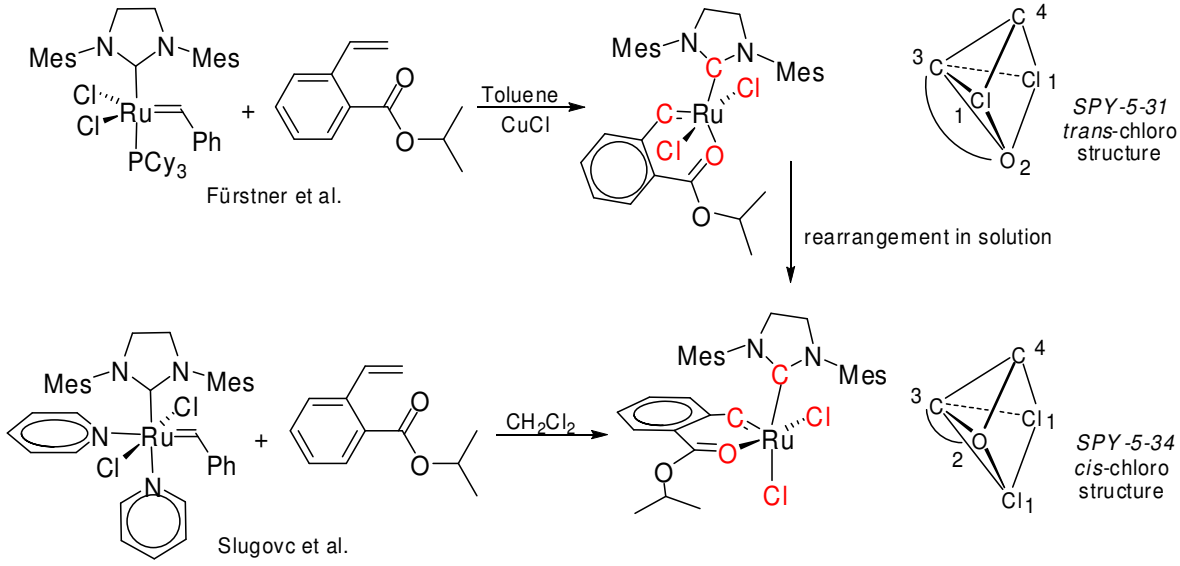

Fig. 17: Synthesis of *trans* - and *cis* – configuration of a chelating complex with an ester ligand

Such configurational changes in similar complexes have already been reported in 2004 by Fürstner's group when he described a rearrangement upon treatment with silica gel.[54]

The obvious strong influence of the starting material on the later stereochemistry of the complex lead to another experiment where **17** was reacted with Neolyst **M2** together with CuCl to give **26a**.

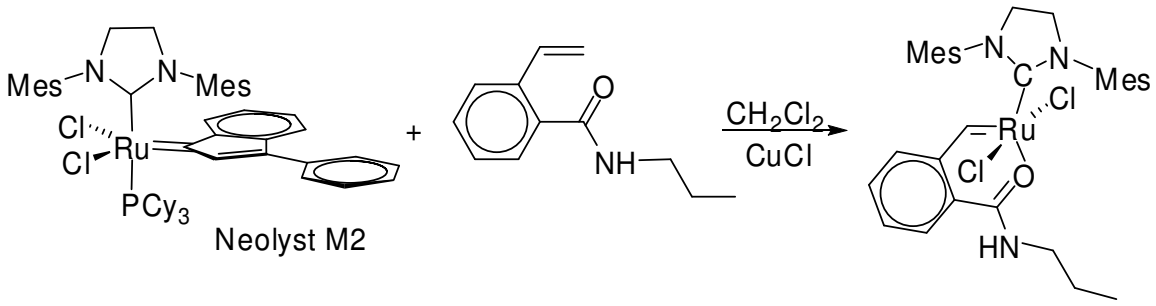

Scheme 13: Synthesis of **26a**

Already the optical appearance of the reaction mixture differed greatly from those of reactions with Neolyst **M3**. After being stirred for one week at room temperature, the turbid, light green solution was filtered in order to remove excess CuCl. Surprisingly, the precipitate turned out to be the now insoluble

[54] Prühs, S.; Lehmann, C.W.; Fürstner, A. *Organometallics*, **2004**, ASAP

product, a light green powder, soluble in MeOH and DMSO. Excess in CuCl form of small glassy beads could be easily removed. ^{1}H-NMR spectroscopy (solvent: CD_3OD) indicated *trans* configuration of the chloro atoms by the position of the carbene peak at 19.46 ppm.

Coalescing or splitting up of the mesityl signals can be explained by possible or partially hindered rotation, respectively. Rotation can be hindered because of steric or electronic reasons. Whereas in the *cis* – chloro configuration a possible π-stacking of one mesityl group with the amide ligand can hinder rotation around the Ru – C bond, in the *trans* – chloro configuration the amide ligand can be a steric obstacle for the rotation of a mesityl group around its own axis. This seems to be the case in **26a**. The corresponding ^{1}H – NMR spectrum is displayed below. The pattern of mesityl merthyl groups is zoomed out. Possible rotations are indicated schematically.

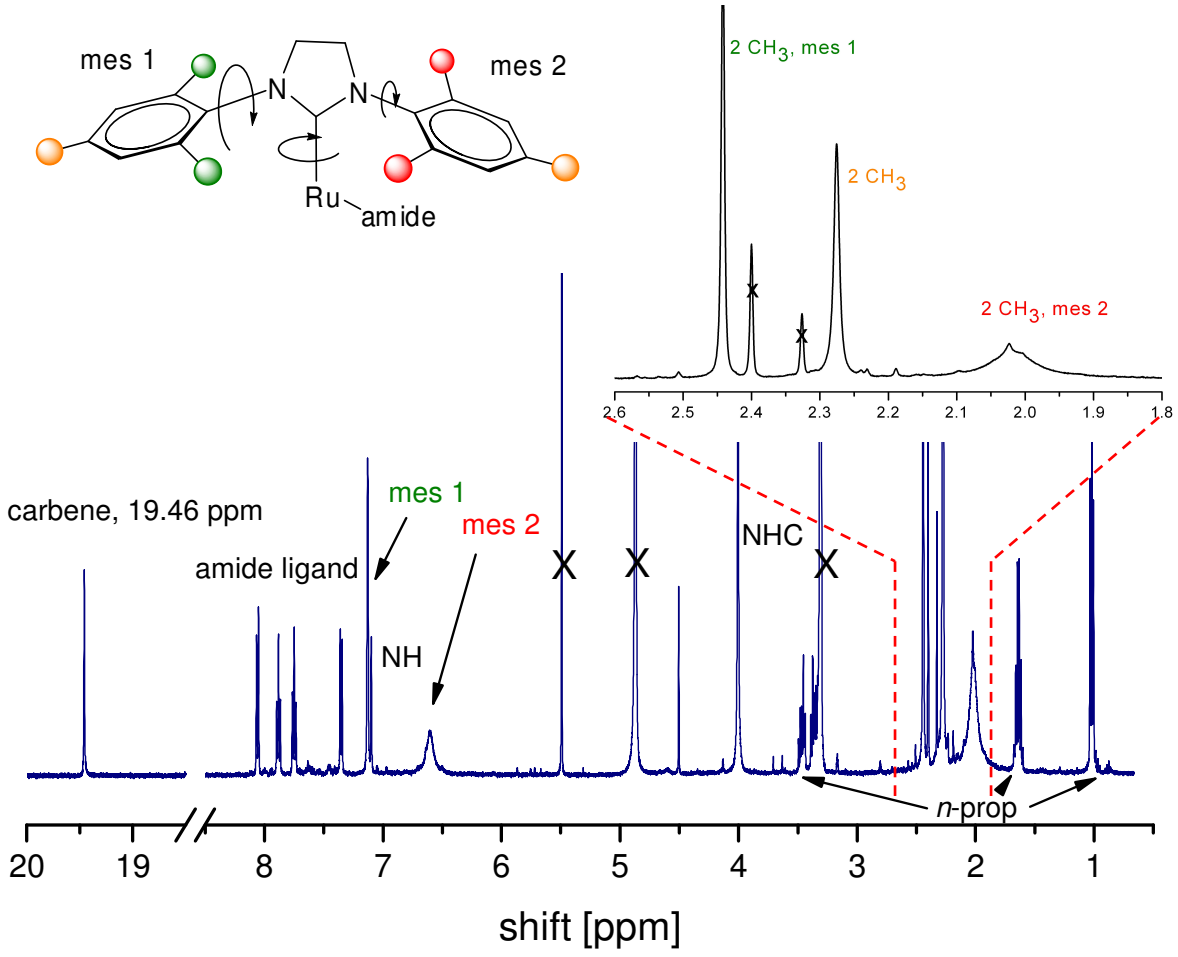

Fig. 18: ^{1}H-NMR spectrum (CD_3OD) of ((**26a**, trans isomer). Solvent peaks (CH_2Cl_2 at 5.49 ppm; H_2O at 4.87 ppm; MeOH at 3.34 ppm) are crossed. All product-related peaks can be assigned.

In the aromatic region a sharp peak at 7.13 and a broad signal at 6.61 ppm, each with the intensity of 2, represent the hydrogen atoms attached at the phenyl core of the mesityl groups. In accordance, the aliphatic region shows three peaks with different shapes, each counting for 2 methyl groups. It can be assumed, that the least hindered rotation is possible at “mes 1”, denoted by the largest rotation arrow and green methyl groups to replace each other. The slightly hindered rotation around the ruthenium bond is indicated by a broader signal of the yellow labelled methyl groups. Rotation around “mes 2” is strongly restricted due to the amide ligand. This causes very broad, hardly coalescing signals. Corresponding methyl groups are coloured in red.

As CD_3OD turned out to be a poor solvent and not suitable for a ^{13}C – spectrum, another series of spectra was recorded in DMSO-d_6. After being in solution for three days, a complete rearrangement to the corresponding *cis* – isomer (26b) was noted.

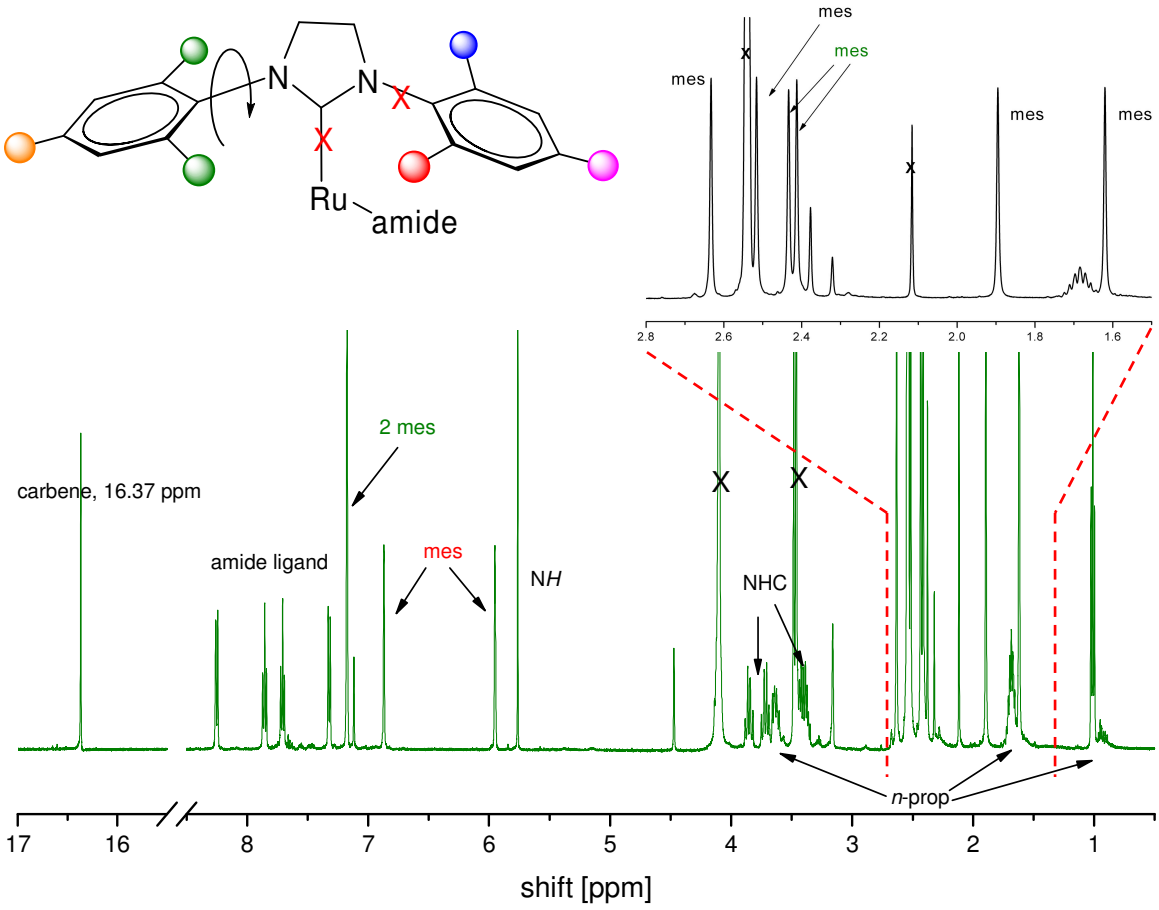

Fig. 19: ^{1}H-NMR spectrum (DMSO-d_6) of **26b**. Solvent peaks (DMSO at 2.45 ppm; H_2O at 3.46 ppm; MeOH at 2.16 and 4.01 ppm) are crossed. All product-related peaks can be assigned.

In the aromatic region, three mesityl signals with intensities of 2 : 1 : 1 imply that one mesityl group can rotate freely whereas the other can not. In the aliphatic region two of six mesityl signals are overlapping partly (coloured in green). The mesityl pattern in the ^{1}H – NMR spectrum reflects possible rotation as shown above. Rotation is hindered because of the π - stacking of a mesityl group and the amide ligand.

In case of ligand **21b**, presumably both configurations were obtained in one pot starting from Neolyst **M3**. They could be separated by column chromatography as their polarity is different. Assignments to the particular isomer were done by studying possible rotations of the NHC ligand and bringing them into accordance with the corresponding NMR-spectrum (compare figure 21).

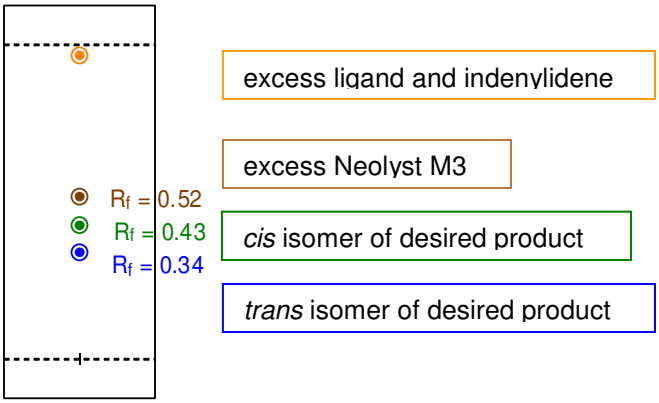

Fig. 20: Obtained TLC of (crude - **27**): silica, CH_2Cl_2:MeOH, 20:1

^{1}H-NMR details of **27a** and **27b** are discussed in the following. A dominant difference in the spectra is given by the position of the carbene signals with an offset of 1.2 ppm.

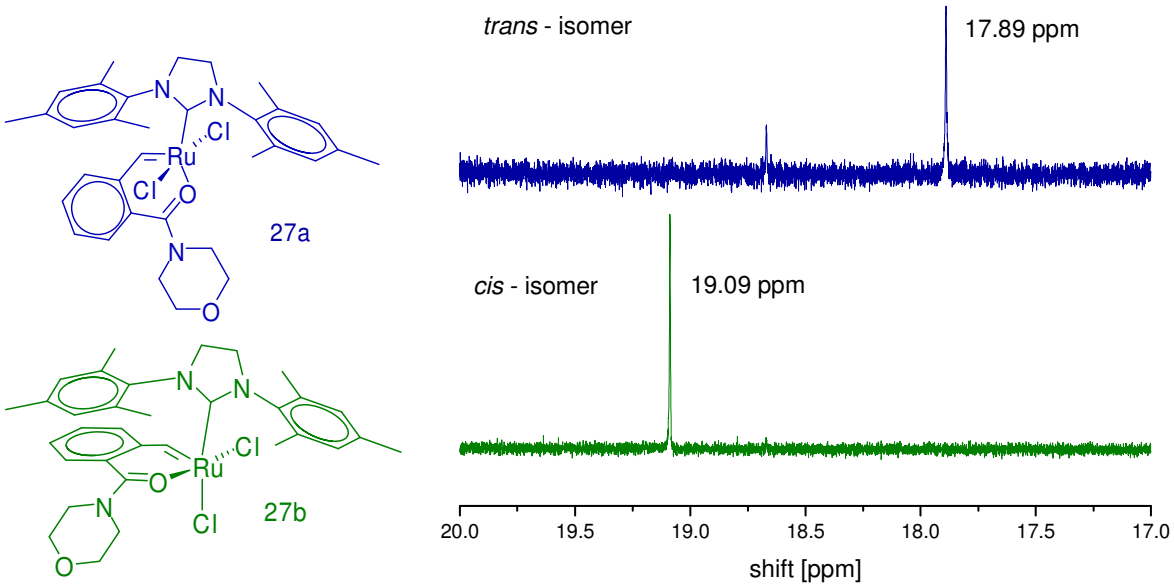

Fig. 21: Detail of 1H-NMR spectra. Comparison of trans – chloro isomer **27a** (blue) and cis – chloro isomer **27b** (green) in the carbene region

In contrast to observations for **26**, the *cis* – isomer's carbene signal is low-field-shifted, compared with the *trans* analogue. In the following table, examples from literature are taken to estimate the probability of this inconsistency. The shift of the more low – shifted isomer is highlighted. No tendency concerning the relative position of the carbene signal of *cis* – and *trans* – isomer in the ^{1}H-NMR spectrum can be noted.

Table 7: Position of the carbene signal [ppm] in 1H-NMR spectroscopy.

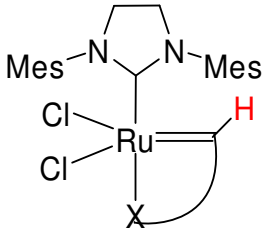

Prototype of the compared complexes: ruthenium – centre with NHC – ligand, 2 chloro ligands in *cis* – or *trans* – configuration, a chelating carbene ligand

Ligand	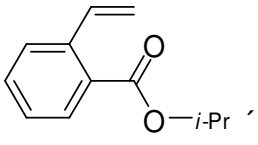 Slugovc[55] Fürstner[56]	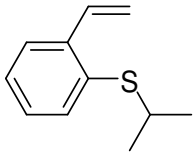 Lemcoff[57]	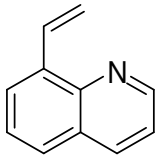 Grela[58]
cis	18.94[a]	17.14 [b]	17.44 [b]
trans	18.82[b]	17.26 [b]	17.06 [b]

Ligand	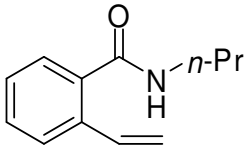 **17**	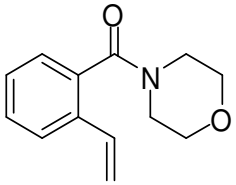 **21**
cis	17.70 [a]	19.09 [a]
trans	19.46 [a]	17.89 [a]

[a] solvent: $CDCl_3$; [b] solvent: CD_2Cl_2;

[55] Slugovc, C.; Perner, B.; Stelzer, F.; Mereiter, K. *Organometallics* **2004**, *23*, 3622.
[56] Fürstner, A.; Thiel, O.R.; Lehmann, C.W., *Organometallics*, **2002**, *21*, 331.
[57] Ben-Asuly, A.; Tzur, E.; Diesendruck, C.E.; Sigalov, M.; Goldberg, I.; Lemcoff, N.G., *Organometallics* **2008**, *27*, 811-813.
[58] Barbasiewicz, M.; Szadkowska, A.; Bujok, R.; Grela, K., *Organometallics*, **2006**, *25*, 3599-3604.

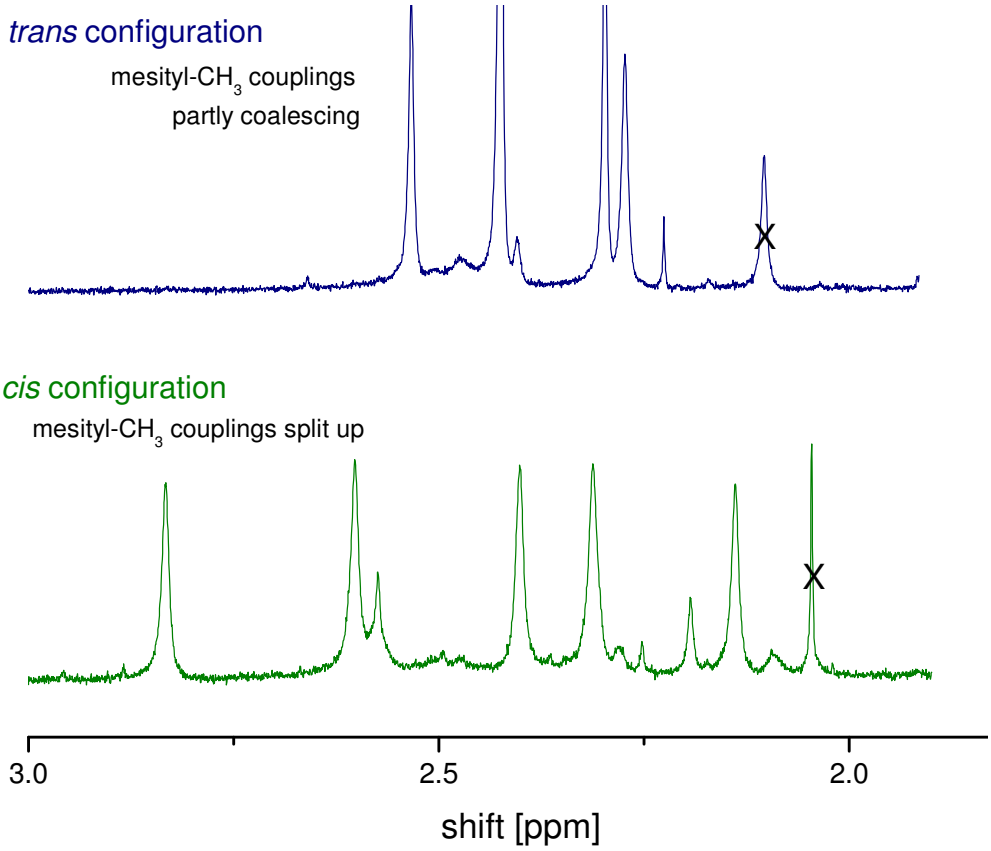

Fig. 22: Aliphatic region of **27a** (blue) and **27b** (green). Rotation possibilities of the NHC ligand is very different for *cis*- and *trans* configuration - in der graphic steht noch couplings….

It can be clearly seen, that due to π-stacking, rotations are far more restricted in the *cis* – isomer, where every single methyl group is visible. In contrast, the orientation of the amide ligand in case of *trans* – chloro configuration enables rotation around the Ru – C bond, and therefore causes coalescing of some signals.

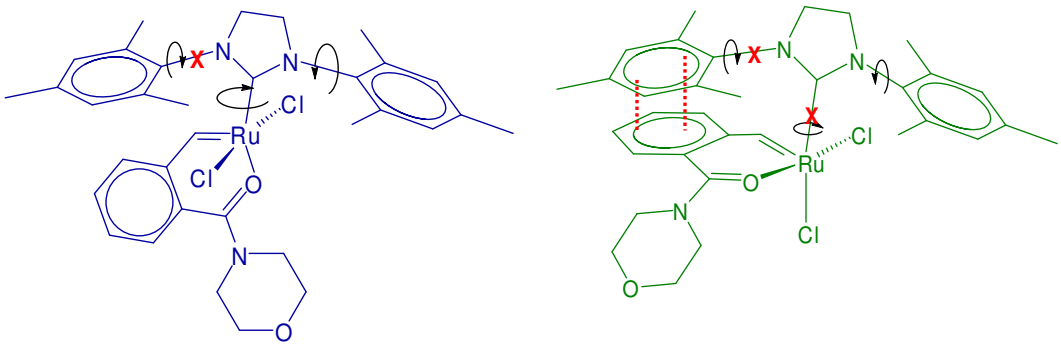

Fig. 23: Possible rotations for **27a** (blue) and **27b** (green).

4 CONCLUSION and OUTLOOK

Within this work, the synthesis and characterisation of ruthenium based metathesis initiators bearing chelating carbene ligands with an amide function is presented.

Complexes were obtained by a carbene exchange reaction of Neolyst **M3** or Neolyst **M2** with the corresponding ligand. A dependency of the chloro ligand's configuration from the way of preparation could be noted for dichloro-(κ^2(C,O)-(2-n-propylamidebenzylidene)-(1,3-bis(2,4,6-trimethylphenyl)4,5-dihydroimidazol-2-ylidene)ruthenium (**24**, **26**). X-ray diffractometry of obtained crystals showed that Neolyst **M3** yielded in the *SPY*-5-34 *cis* isomer **24**. Bond lengths and bond angles were found to be similar to a comparable ester derivative (**25**). In contrast, the reaction of Neolyst **M2** with the according ligand in presence of CuCl produced the corresponding *SPY*-5-31 *trans* isomer **26a**, which is insoluble in CH_2Cl_2, but in solution of DMSO quickly rearranges to *SPY*-5-34 *cis* configuration **26b**, as determined by NMR – spectroscopy.

Complex **27** which is bearing a morpholino functionalized amide ligand was presumably obtained in *cis* and *trans* configuration in one pot starting from Neolyst **M3**. The isomers could be separated by column chromatography. Still, NMR spectra showed an oversupply of signals in all regions. No crystals could be obtained from ether diffusion.

Summarizing it can be said that the synthesis of ruthenium based metathesis initiators bearing chelating carbene ligands with an amide function seems to be more controllable and therefore more promising when starting from Neolyst **M2** than from Neolyst **M3**.

Characterization of the complexes concerning their metathesis capability and thermo-switchable behaviour could not be accomplished in this work. Another future task is the further investigation of alternative amide ligands like the diethyl derivative **20b**.

5 EXPERIMENTAL PART

5.1 Chemicals

All chemicals for ligand synthesis were purchased from commercial sources (Sigma Aldrich, Fluka or Alfa Aesar) and used without further purification. Neolyst **M2** and Neolyst **M3** were obtained from UMICORE AG. Solvents and auxiliary materials were used as purchased if not mentioned otherwise.

5.2 Thin layer chromatography (TLC)

TLC sheets: silica gel 60 F_{254} on aluminium (Merck). Visualization was done by UV light irradiation (254 and 365 nm) or dipping into an aqueous solution of $KMnO_4$ (0.5%).

5.3 Nuclear Magnetic Resonance Spectroscopy (NMR)

NMR spectroscopy was performed on a VARIAN INOVA 500 MHz spectrometer. ^{1}H spectra were recorded at 499.764 MHz whereas ^{13}C $\{^{1}H\}$ spectra were recorded at 125.665 MHz. Deuterated solvents were obtained from Cambridge Isotope Laboratories, Inc., remaining peaks were referenced according to literature.[59] Peak shapes are indicated as follows: s (singlet), d (doublet), dd (doublet of doublets), t (triplet), q (quadruplet), m (multiplet), b (broad), bs (broad singlet).

5.4 X-ray diffractometry

The obtained X-ray structure was measured on Bruker “Kappa APEX-2“ diffractometer by Kurt Mereiter at Vienna, University of Technology.

[59] Gottlieb H. E., Kotlyar A., Nudelman A. *J. Org. Chem.* **1997**, *62*, 7512.

5.5 Syntheses of 2-Bromobenzamide derivatives

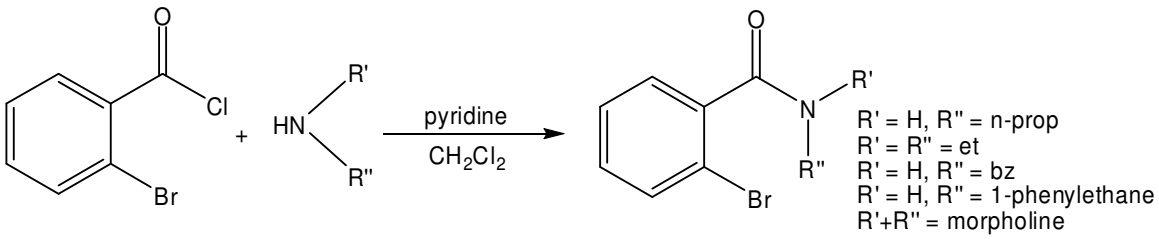

Scheme 14: General scheme of performed amidation reactions

5.5.1 2-Bromo-N-propylbenzamide (17a)

2-Brombenzoylchloride (581 mg, 2.66 mmol, 1 eq), pyridine (628 µL, 3 eq) were dissolved in 10 mL dry, degassed CH_2Cl_2 in a Schlenk flask and stirred under argon atmosphere at 0 °C. *n*–propylamine (243 µL, 1.1 eq) was added slowly. The mixture was brought to room temperature and stirred overnight. Progress of the reaction was monitored via TLC. For workup, the solution was washed with HCl, and $NaHCO_3$, three times each. The organic layer was dried with Na_2SO_4. Removing the solvent in vacuo yielded a light yellow solid which was then purified by flash column (SiO_2, cyclohexane/ethyl acetate 3:1). Yield: 264 mg (54%). TLC: (silica, cyclohexane/ethyl acetate 3:1, R_f = 0.22)

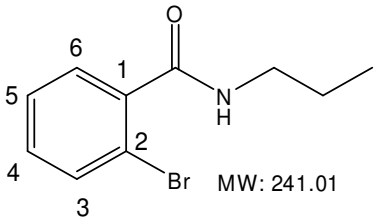

^{1}H-NMR (δ, 20°C, $CDCl_3$, 500 MHz): 7.56 (d, ph^6), 7.50 (d, ph^3), 7.34, 7.25 (2t, 2H ph^{4,5}), 6.033 (s, N*H*), 3,41 (q, 2H, NHC*H*$_2$), 1.65 (hex, 2H, CH_2C*H*$_2$$CH_3$), 0.99 (t, 3H, C*H*$_3$).

^{13}C-NMR (δ, 20°C, $CDCl_3$, 500 MHz):169.44, 135.80, 135.79, 134.66, 130.13, 127.62, 127.47, 126.34, 116.78, 41.81 ($NHCH_2$), 22.98, (CH_2*C*H_2CH_3) 11.55 (CH_3).

5.5.2 2- N-Benzyl-2-bromobenzamide (18a)

18a was prepared similar to **17a** using 2-brombenzoylchloride (522 mg, 2.40 mmol, 1 eq), pyridine (590 µL, 3 eq), benzylamine (290 µL, 1.1 eq) and 17 mL of dry and degassed CH_2Cl_2. Upon addition of the amine, the clear solution turned milky white. After workup a yellow solid was obtained, which was redissolved in a little CH_2Cl_2. The solution was overlaid with *n*-pentane which allowed a white flaky solid to precipitate overnight. Yield: 355 mg (51%). TLC: (silica, cyclohexane/ethyl acetate 3:1); R_f = 0.30

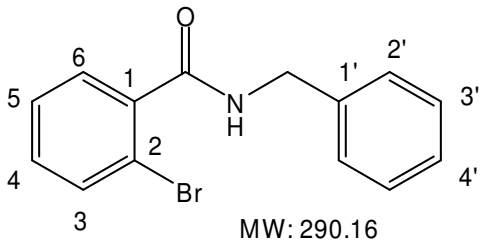

^{1}H-NMR (δ, 20°C, CDCl3, 500 MHz): 7.58(2d, 2H, ph^{4,5}), 7.39-7.27 (3m, 7H, ph^{1,4},bz$^{2'-6'}$), 6.23 (s, N*H*), 4.66 (d, 2H, CH_2).

^{13}C-NMR (δ, 20°C, CDCl3, 500 MHz): 207.31, 138.00, 133.74, 131.67, 129.99, 129.12 (2C), 128.36 (2C), 128.05, 127.92, 119.63, 44.60, 31.29.

5.5.3 2-Bromo-N-(1-phenylethyl)benzamide (19a)

19a was prepared analogously to **18a** using 2-brombenzoylchloride (556 mg, 2.55 mmol, 1 eq), pyridine (623 µL, 3 eq), (S)–1–phenylethanamine (358 µL, 1.1 eq) and 18 mL of dry and degassed CH_2Cl_2. Upon addition of the amine, the solution turned slightly yellow. Progress was monitored via TLC. After 6 h another 50 µL of amine (0.2 eq.) were added before the reaction mixture was allowed to stir overnight. After workup a yellow oil was obtained, which was redissolved in a little CH_2Cl_2. The solution was overlaid with *n*-pentane which caused the precipitation of white solid. Yield: 510 mg (66%). TLC: (silica, cyclohexane/ethyl acetate 3:1); R_f = 0.42)

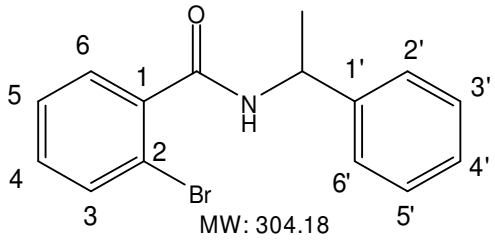

^{1}H-NMR (δ, 20°C, $CDCl_3$, 500 MHz): 7.57, 7.54 (2d, 2H, ph^{3,6}), 7.42-7.24 (3m, 7H, ph^{5,4},bz$^{2'-6'}$), 6.19 (s, N*H*), 5.35 (m, C*H*), 1.63 (d, 3H, CH_3).

^{13}C-NMR (δ, 20°C, CDCl3, 500 MHz): 166.92, 142.91, 138.10, 133.68, 131.58, 130.04, 129.07 (2C), 127.91, 127.88, 126.69 (2C), 119.59, 49.95, 21.94.

5.5.4 Bromo-N,N-diethylbenzamide (20a)

20a was prepared analogously to **17a** using 2-brombenzoylchloride (501 mg, 2,29 mmol, 1 eq), pyridine (543 µL, 3 eq) and diethyl amine (264 µL, 1.1 eq) and 10 mL of dry and degassed CH_2Cl_2. When the amine was added, the solution turned into deep yellow which slowly changed to red. Purification yielded 240 mg (55%) of a red oily liquid. TLC: (silica, cyclohexane/ethyl acetate 3:1, R_f = 0.26)

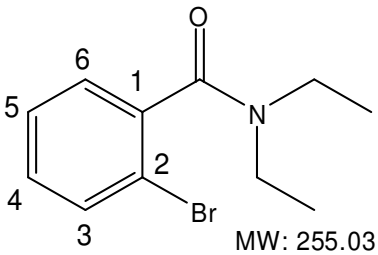

MW: 255.03

^{1}H-NMR (δ, 20°C, $CDCl_3$, 500 MHz): 7.56 (d, ph^6), 7.34 (m, 1H ph^4), 7.23 (m, 2H ph^{3,5}), 3.84, 3,34 (2m, 2H, NC*H*H)*, 3.15 (m, 2H, NCH_2)*, 1.27 (t, 3H, NCHHCH_3), 1.06 (t, 3H, NCH_2CH_3).$^{*)}$ can not be distinguished

^{13}C-NMR (δ, 20°C, $CDCl_3$, 500 MHz): 168.70 (*C*=O); 139.70 (ph^3), 132.98 (ph^5), 130.16 (ph^4), 127.77 (ph^6), 119.48 (ph^2), 42.90 (N*C*HH), 39.14 (N*C*H_2), 14.15 (NCHH*C*H_3), 12.77 (NCH_2*C*H_3).

5.5.5 2-Bromophenyl(morpholino)methanone (21a)

21a was prepared similar to **17a** using 2-brombenzoylchloride (649.3mg, 2.98 mmol, 1 eq), pyridine (729µL, 3 eq), morpholine (389µL, 1.5 eq) and 20 mL of dry and degassed CH_2Cl_2. After reacting overnight, the crude product was filtered in order to remove excess pyridinium chloride precipitate. After aqueous workup purification on a silica column was performed (cyclohexane/ethyl acetate, 8:1 to 2+1) and white solid was obtained. Yield: 466mg (58%). TLC: (silica, cyclohexane/ethyl acetate 1+1); R_f = 0.36).

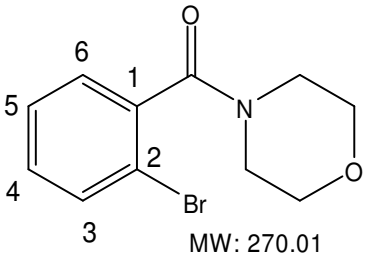

MW: 270.01

^{1}H-NMR (δ, 20°C, $CDCl_3$, 500 MHz): 7.47 (d, ph^6); 7.36 (t, ph^5), 7.26-7.24 (m, 2H, ph^{3,4}), 3.90-3.75 (m, 4H, CH_2OCH_2), 3.72 (ddd, 1H, C*H*HNCH_2), 3.58 (ddd, 1H, CH*H*NCH_2), 3.28 (ddd, 1H, CH_2NC*H*H), 3.19 (ddd, 1H, CH_2NCH*H*).

^{13}C-NMR (δ, 20°C, CDCl3, 500 MHz):167.61, 137.45, 132.73, 130.33, 127.68, 127.62, 119.02, 66.64, 66.55, 47.03, 41.88.

5.6 Syntheses of 2-Vinylbenzamide derivatives

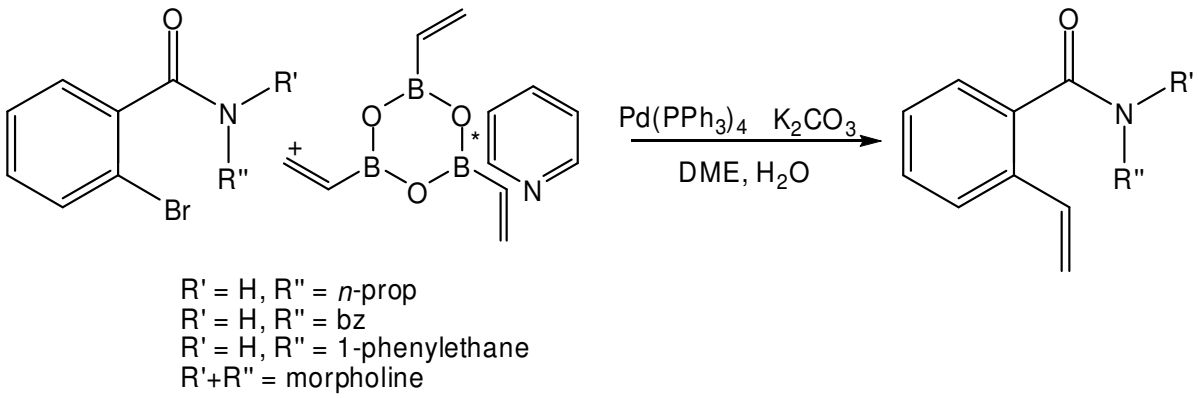

Scheme 15: General scheme of vinylation via Suzuki coupling

5.6.1 N-Propyl-2-vinylbenzamide (17b)

2-Brom-N-propylbenzamide **17a** (260 mg, 1.08 mmol, 1 eq), vinylboronic anhydrid pyridine complex (312 mg, 1.2 eq) and K_2CO_3 (300 mg, 2 eq.) were dissolved in a mixture of degassed DME (6 mL) and H_2O (2 mL) in a Schlenk flask, heated to reflux (90 °C) and stirred under argon atmosphere. $Pd(PPh_3)_4$ (25 mg, 2 mol%) was added. The mixture was refluxed overnight and then cooled down to ambient temperature. The formation of a vinyl functionality was controlled via TLC upon the appearance of a bright yellow spot after visualization by means of aqueous $KMnO_4$ solution. 10 mL of water were added, before the solution was extracted with Et_2O twice. After drying with Na_2SO_4, the organic solvent was removed in vacuo. Purification on a silica flash column (cyclohexane/ethyl acetate 3:1) yielded a light yellow solid. Yield: 172 mg (84%).
TLC: (cyclohexane/ethyl acetate 3:1); R_f = 0.30

^{1}H-NMR (δ, 20 °C, $CDCl_3$, 500 MHz): 7.50 (d, ph^6), 7.39 (d, ph^3), 7.33, 7.23 (2t, 2H $ph^{4,5}$), 6.98 (q, PhC*H*CH_2), 6.73 (s, N*H*), 5.65 (d, J_{HH} = 17.5Hz CHC*H*^{trans}H), 5.28 (d, J_{HH} = 6.5 Hz, CHCH*H*^{cis}), 3,34 (q, 2H, NHC*H*$_2$), 1.56 (hex, 2H, CH_2C*H*$_2$), 0.92 (t, 3H, C*H*$_3$).

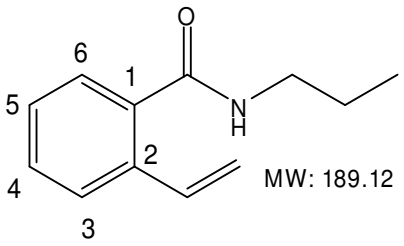

5.6.2 N-Benzyl-2-bromobenzamide (18b)

18b was prepared analogously to **17b**, using **18a** N-benzyl-2-bromobenzamide (298 mg, 1.03mmol, 1eq.), vinylboronic anhydrid pyridine complex (296 mg, 1.2eq), K_2CO_3 (385 mg, 2.7 eq.) and $Pd(PPh_3)_4$ (28 mg, 2 mol%). Workup as described above followed the reaction. Purification on a silica column yielded a light yellow solid. Yield: 185mg (76%). TLC: (cyclohexane/ethyl acetate 3:1); R_f = 0.40.

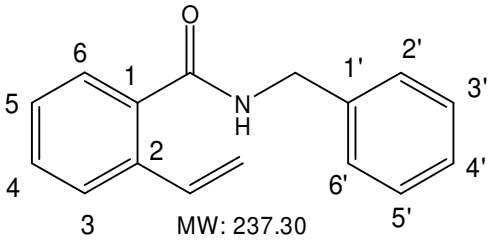

^{1}H-NMR (δ, 20°C, $CDCl_3$, 500 MHz): 7.56(d, ph^6), 7.48 (d, ph^3), 7.40 (t, ph^5), 7.35-7.29 (3m, bz$^{2'\text{-}6'}$, ph^4), 7.07 (q, PhC*H*), 6.05 (s, N*H*), 5.70 (d, CHC*H*^{trans} H), 5.34 (d, CHCH*H*^{cis}), 4.64 (d, 2H, NHCH_2).

^{13}C-NMR (δ, 20°C, CDCl3, 500 MHz): 169.51, 138.31, 136.30, 135.47, 134.84, 130.60, 129.13 (2C), 128.21 (2C), 128.07, 127.99, 127.73, 126.69, 117.19, 44.48.

5.6.3 N-(1-Phenylethyl)-2-vinylbenzamide (19b)

19b was prepared similar to **17b**, using 2-bromo-N-(1-phenylethyl)-benzamide (**19a**) (442 mg, 1.45 mmol, 1 eq), vinylboronic anhydrid pyridine complex (420 mg, 2 eq), K_2CO_3 (580 mg, 2.9 eq) and $Pd(PPh_3)_4$ (33 mg, 2 mol%) in a solvent mixture of DME (8 mL) and H_2O (3 mL). After workup the crude product was conducted to column chromatography (cyclohexane/ethyl acetate 5:1). 210 mg of yellow solid were isolated (yield: 58%). TLC: (cyclohexane/ethyl acetate 3:1); R_f = 0.43

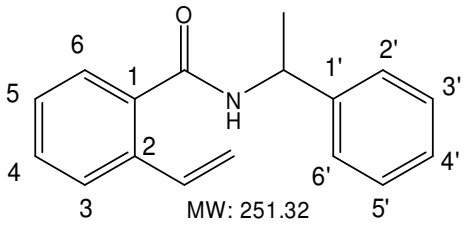

^{1}H-NMR (δ, 20°C, $CDCl_3$, 500 MHz): 7.54 (d, ph^6), 7.45 (d, ph^3), 7.37-7.27 (2m, 7H, bz$^{2'\text{-}6'}$, ph^{4,5}), 7.00 (q, PhC*H*), 6.02 (s, N*H*), 5.68 (d, PhCHC*H*^{trans} H), 5.34 (d, PhCHCH*H*^{cis}), 5.32 (m, NHC*H*CH_3), 1.60 (d, 3H CH_3).

^{13}C-NMR (δ, 20°C, $CDCl_3$, 500 MHz):168.71, 143.25, 136.20, 135.66, 134.85, 130.50, 129.08 (2C), 128.06, 127.82, 127.73, 126.65, 126.55 (2C), 117.12, 49.67, 22.15.

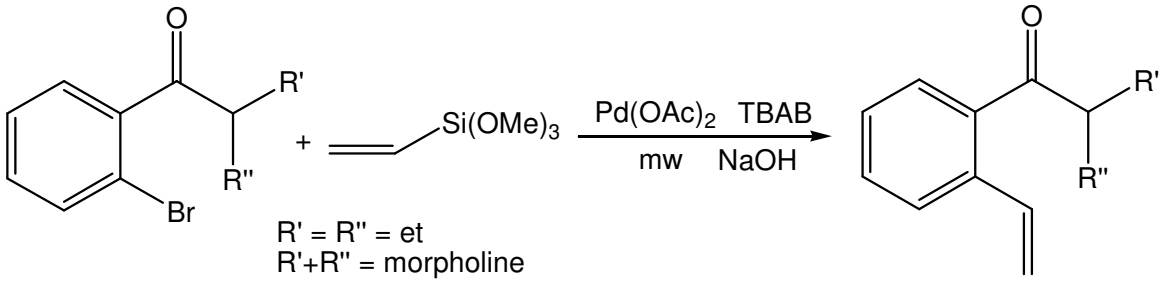

Scheme 16: General procedure for a Hiyama coupling

5.6.4 2-Vinyl-N,N-diethylbenzamide (20b)

10 mL of aqueous NaOH solution (0.5 M) were put into a microwave Teflon® liner together with a stirring bar. 2-bromo-N,N-diethylbenzamide (**20a**) (168 mg,0.658 mmol; 1 eq) and tetrabutylaminobromide (TBAB, 106 mg, 0,5 eq) were added under vigorous stirring. Trimethoxysilane (250 µL, 2.5 eq) and $Pd(OAc)_2$ (12 mg; 8 mol%) were added just before the tube was sealed and put into the microwave together with three blanks to run the following temperature program:

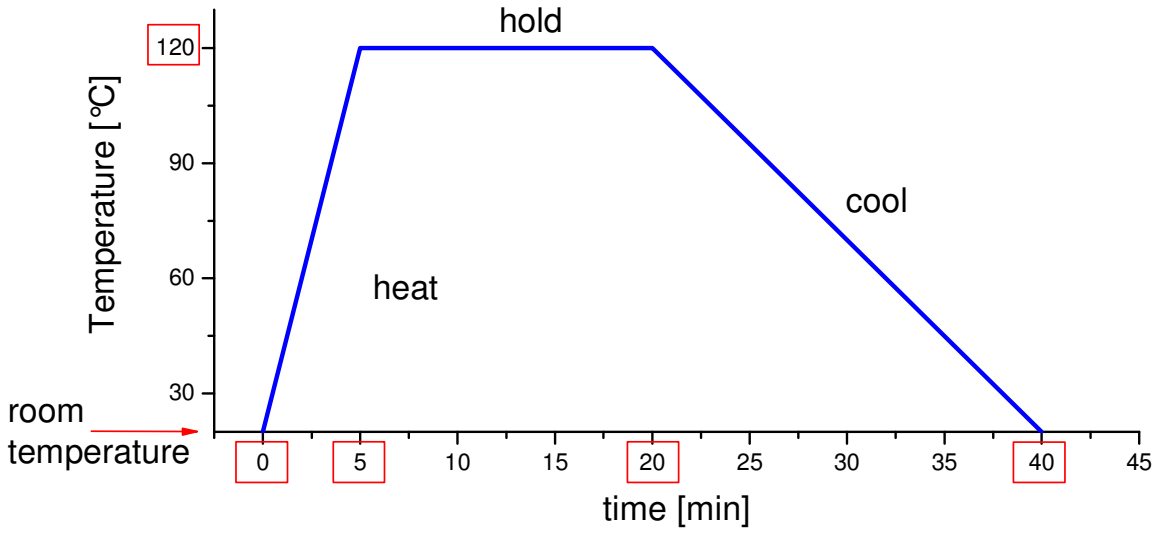

Fig.24: Microwave program applied for all performed Hiyama reactions

For work up, the reaction mixture was filtered in order to remove the catalyst's degradation products, and the crude product was extracted with Et_2O three times. After drying over Na_2SO_4, the solvent was removed in vacuo. Light yellow oil was obtained. No further purification steps were necessary. Yield: 62 mg (61%). TLC: (silica, solvent: cyclohexane/ethyl acetate 3/1); R_f= 0.58.

^{1}H-NMR (δ, 20°C, CDCl3, 500 MHz): 7.58 (d, ph^6), 7.34 (t, ph^4), 7.29 (t, ph^5), 7.20 (d, ph^3), 6.72 (dd, PhC*H*), 5.75, (d, HC=CH*H*^{trans}), 5.30 (d, HC=C*H*^{cis}H), 3,54 (bd, 2H, NC*HH*CH$_3$), 3.10 (2d, 2H, NC*H*$_2$), 1.30, 1.00 (2t, 6H, 2C*H*$_3$).

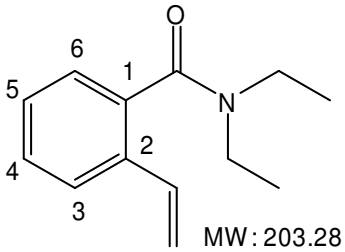

MW: 203.28

^{13}C-NMR (δ, 20°C, CDCl3, 500 MHz):170.38, 136.22, 134.07, 133.59, 128.76, 127.84, 126.10, 125.35, 116.36, 42.88, 38.92, 14.01, 12.93.

5.6.5 Morpholino(2-vinylphenyl)methanone (21b)

21b was prepared analogously to **20b**, using 2-bromophenyl(morpholino) methanone (**21a**) (101.3 mg, 0.375 mmol, 1 eq), TBAB (64.1, 0.5 eq), trimethoxyvinylsilane (148 µL, 2.5 eq) and $PdOAc_2$ (9.0 mg, 8 mol%) in 10 mL of NaOH (0.5 M). Workup as described above yielded an opaque yellow oil. Yield: 56 mg (69%). TLC (silica, solvent: cyclohexane/ethyl acetate 3+1); R_f = 0.15

^{1}H NMR (δ, 20°C, $CDCl_3$, 500 MHz): 7.59 (d, ph^6); 7.37 (t, ph^4), 7.31 (t, ph^5), 7.22 (d, ph^3), 6.75 (dd, PhC*H*), 5.76 (d, HC=CH*H*^{trans}), 5.36 (d, HC=C*H*^{cis}H), 3.839-3.770 (m, 4H, C*H*$_2$OC*H*$_2$), 3.55, 3.187 (2t, 2*2H, C*H*$_2$OC*H*$_2$).

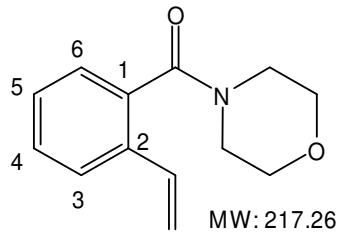

MW: 217.26

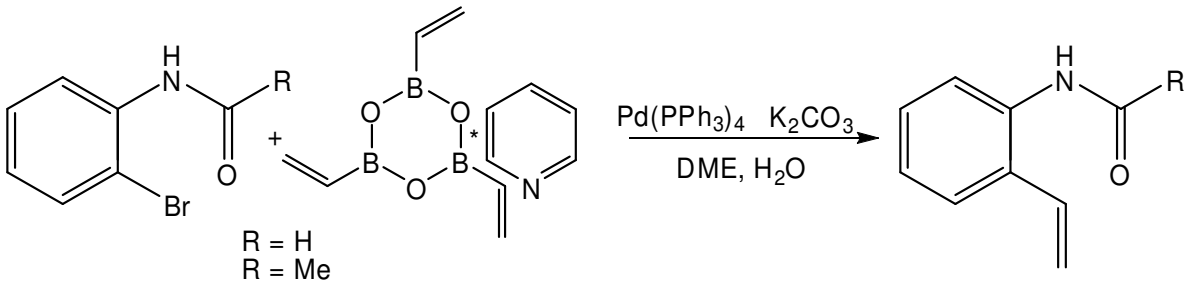

Scheme 17: Suzuki coupling of anilide derivatives

5.6.6 N-(2-Vinylphenyl)formamide (22)

N-(2-bromophenyl)formamide (247.7 mg, 1.23 mmol; 1 eq), vinylboronic anhydrid pyridine complex (389.4 mg, 1.3 eq) and K_2CO_3 (516.1 mg, mmol, 3 eq.) were dissolved in a mixture of degassed DME (12 mL) and H_2O (4 mL) in a

Schlenk flask, heated to reflux (90 °C) and stirred under argon atmosphere. $Pd(PPh_3)_4$ (29 mg, 2 mol%) was added. The mixture was refluxed overnight and then cooled down to ambient temperature. 10 mL of water were added before the crude product was extracted with, Et_2O twice. The organic layer was dried over Na_2SO_4 and the solvent was then removed in vacou. Purification on a silica column (cyclohexane/ethyl acetate 2+1) afforded light yellow crystals. Yield: 108 mg (46%). TLC: (cyclohexane/ethyl acetate 2+1); R_f = 0.38

According to ^{1}H.NMR spectroscopy, the substrate as well as the product exists in a tautomeric mixture (see scheme below). NMR data for the formimidic acid are labelled with "*"

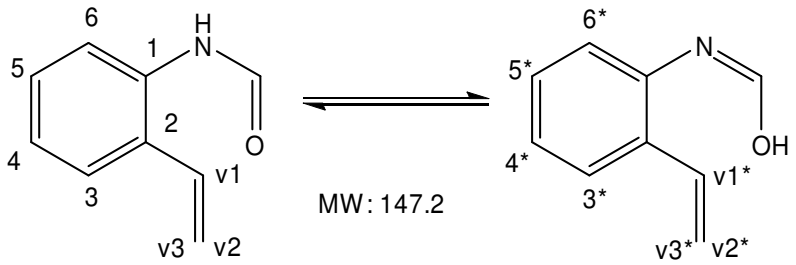

N-(2-vinylphenyl)formamide *N*-(2-vinylphenyl)formimidic acid

Scheme 18: Tautomerism of N-(2-Vinylphenyl)formaide and N-(2-Vinylphenyl)formimidic acid; According to 1H-NMR, ratio = 1:1.5.

^{1}H-NMR (δ, 20°C, $CDCl_3$, 500 MHz): 8.51 (d, 1.5H, N=C*H**), 8.45 (s, 1H, N(C=O)*H**), 7.96 (d, 1H, ph^6), 7.51 (d, 1.5H, ph^{6*}), 7.42 (d, 1H, ph^3), 7.35-7.30 (2bs, N*H*, O*H**), 7.31-7.15 (3m, $ph^{4,5,3*,4*,5*}$), 6.81 (m, 2.5H, $v^{7,7*}$), 5.7 (2d, 2.5H $v^{3,3*}$), 5.45 (2d, 2.5H, $v^{2,2}$).

^{13}C-NMR (δ, 20°C, CDCl3, 500 MHz): 163.61*; 159.36, 133.74*, 133.46, 132.15, 131.70*, 131.35*, 130.19, 129.08*, 128.81, 127.66*, 127.31, 126.65*, 125.88, 123.59, 122.06*, 118.90, 188.55*.

5.6.7 N-(2-Vinylphenyl)acetamide (23)

23 was similar prepared to **22**, following conditions of Cottineau et al.[60] N-(2-bromophenyl)acetamide (200 mg, 0.932 mmol, 1 eq.) vinylboronic anhydrid

[60] Cottineau, B.; Kessler, A.; O'Shea, D.F.; *Org. Synth.*, **2006**, *83*, 45-48.

pyridine complex (238.8 mg, 3 eq) and K_2CO_3 (129.8 mg, 1eq.) were dissolved in a mixture of degassed DME (12 mL) and H_2O (4 mL) and brought to reflux under argon atmosphere. $Pd(PPh_3)_4$ (21.6 mg, 2 mol%) were added before the mixture was allowed to stir overnight. The crude product was filtered and extracted with Et_2O, aqueous workup with diluted HCl (10%) and saturated $NaHCO_3$ solution followed. The organic layer was dried over Na_2SO_4 and the solvent was then removed in vacuo. Purification on a silica column (Et_2O:Cy 9+1) afforded a pale yellow solid. Yield: 81 mg (54%). TLC: (Cy/EtOAc 3+1); R_f = 0.39

^{1}H-NMR (δ, 20°C, $CDCl_3$, 500 MHz): 7.82 (d, ph^6), 7.42 (d, ph^3), 7.29 (t, ph^5), 7.12 (t, ph^4), 7.10 (bs, N*H*), 6.79 (q, PhC*H*), 5.67 (d, HC=CH*H*^{trans}), 5.42 (d, HC=C*H*^{cis}H), 2.21 (2, 3H, C*H*$_3$).

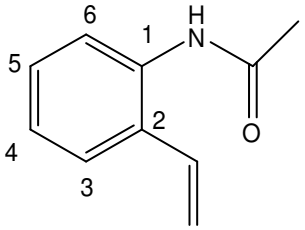

MW: 161.20

5.7 Syntheses of Ru(II) – Complexes

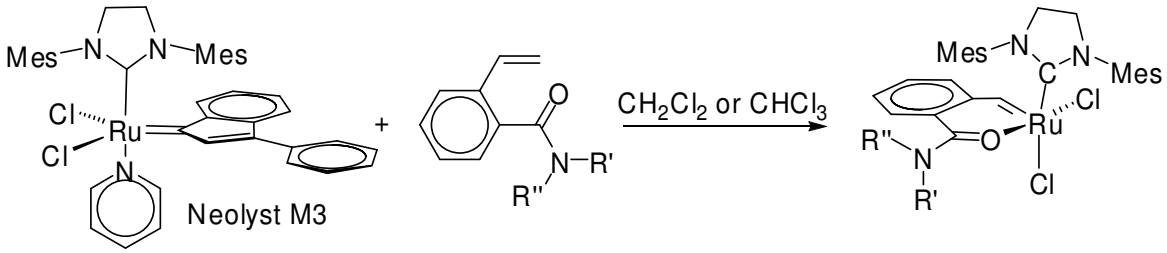

Scheme 19: Typical procedure for the formation of a new Ruthenium complex

Only one of the prepared complexes, **24**, yielded crystals that were appropriate to single crystal X-ray diffractometry. As it showed the expected *cis* configuration of the chloro ligands, the other complexes are assumed to exhibit the same stereochemistry with exception of **26a** which was prepared differently.

5.7.1 (SPY-5-34)-Dichloro-(κ^2 (C,O) - (2-n-propylamidebenzylidene)-(1,3-bis (2,4,6 - trimethylphenyl) 4, 5 – dihydroimidazol - 2 - ylidene) ruthenium (24)

Neolyst **M3** (100 mg, 0.134 mmol, 1 eq) and *n*-propyl-2-vinylbenzamide (**17b**) (38 mg, 1.5 eq) were put into a small Schlenk flask which was then flushed with argon. 6 mL of degassed $CHCl_3$ were added with a syringe. The reaction mixture was allowed to stir at room temperature for 18 h. During this time the colour turned from brownish red to deep green. The solvent was removed by evacuation. The residual solid was washed with *n*-pentane in order to remove excess ligand and compensated methylene-3-phenylindene. The latter was isolated by column chromatography (Cy: EtOAc, 5:1) and identified by NMR spectroscopy (^{1}H, ^{13}C, DEPT). ^{1}H-NMR spectroscopy of the remaining dark green powder showed as well couplings of the desired product as many impurities. Ether diffusion into a concentrated CH_2Cl_2 – solution of the powder, carried out under argon atmosphere, furnished emerald green crystals. It was not possible to record an NMR spectrum of these, as they turned out to be not soluble in any tested solvent. Yield: not determined. TLC: (silica, CH_2Cl_2: MeOH, 20:1); greenish trace up to R_f = 0.51. NMR spectra were obtained from (**26b**) after a rearrangement of in DMSO-d_6 in the NMR tube.

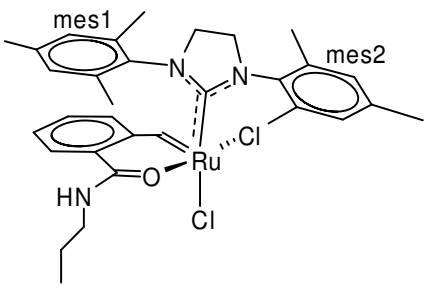

^{1}H-NMR (δ, 20°C, DMSO-d6, 500 MHz): 16.37 (s, Ru=C*H*), 8.25 (d, ph^6), 7.86 (t, ph^4), 7.70 (t, ph^5), 7.32 (d, ph^3), 7.17 (7.13 (s, 2H mes2), 6.87 (s, 1H, mes1), 5.95 (s, 1H mes1), 5,76, (s, NH), 3.86 (q, 1H, H_2Imes), 3.77 (q, 1H, H_2Imes), 3,65 (m, 1H, NHCH*H*), 3.45-3,35 (m, 2H+1H, H_2Imes, NHCH*H*), 2.63 (s, 3H, CH_3^{mes}), 2.52 (s, 3H, CH_3^{mes}), 2,43 (s, 3H,CH_3^{mes}), 2.41 (s, 3H, CH_3^{mes}), 1.90 (s, 3H, CH_3^{mes}), 1.68 (m, 2H, C*H*$_2$CH$_3$), 1.62 (s, 3H, CH_3^{mes}), 1.01 (t, 3H, CH_2CH_3).

^{13}C-NMR (δ, 20°C, DMSO-d6, 500 MHz): 204.39 (C=O), 171.25 (NCN), 143.03, 138.31, 137.67, 137.63, 137.20, 136.93, 136.72, 136.08, 135.62, 135.43, 132.88, 131.28, 130.31, 129.69, 129.49, 129.43, 128.67, 128.02, 125.51 (18 ph +1 n.d.) 52.76, 50.28 (NCCN), 42.62 (NH*C*CH$_2$), 21.79 ($CH_2CH_2CH_3$), 20.58 , 20.45, 18.46, 18.23, 17.47, 17.15, 16.62 (6x CH_3^{mes}), 11.45 (CH_2CH_3).

5.7.2 (SPY-5-31)-Dichloro-(κ^2 (C,O) - (2-*n*-propylamidebenzylidene)-(1,3-bis (2,4,6-trimethylphenyl) 4, 5 – dihydroimidazol-2-ylidene) ruthenium (26a)

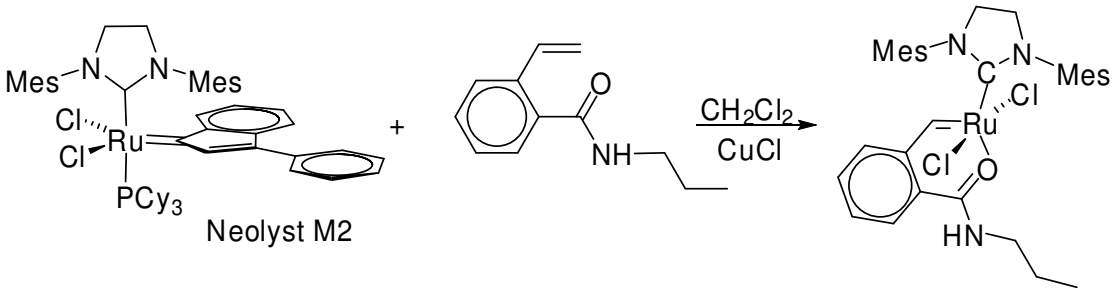

Scheme 20: Reaction procedure for a carbene exchange reaction starting from Neolyst **M2**

Neolyst **M2** (100 mg, 0.105 mmol, 1 eq), *n*-propyl-2-vinylbenzamide (**17a**) (30 mg, 1.5 eq) and 12 mL of degassed and dry CH_2Cl_2 as solvent were separately put into a glovebox and combined in a screw lid vial with a stirring bar. CuCl (13 mg, 1.3 eq) were added. The reaction mixture was allowed to stir for one week, whilst light green powder precipitated. The product was filtered, dried in vacuo, and directly submitted to NMR spectroscopy without any further purification steps. After some solubility tests, MeOD was found to be a moderate solvent, suitable for ^{1}H-NMR.

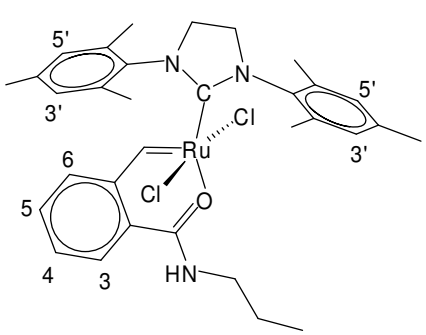

^{1}H-NMR (δ, 20 °C, CD_3OD, 500 MHz): 19.46 (s, Ru=C*H*), 8.06 (d, ph^6), 7.88 (t, ph^4), 7.75 (t, ph^5), 7.35 (d, ph^3), 7.13 (s, 2H mes$^{3'}$), 7.10 (s, NH), 6.61 (bs, 2H, mes$^{5'}$), 4.00 (2, 4H, NCH_2CH_2N), 3.45 (m, NHC*H*H), 3.37 (m, NHCH*H*), 2.44 (s, ~6H, mes, 2CH_3), 2,28 (s, ~6H, mes, 2CH_3), 2.02 (bs, 6H, 2CH_3), 1.63, (hex, 2H, C$H_2$$CH_3$), 1.02 (t, CH_2CH_3).

The coordinating solvent DMSO is a much better solvent. A complete rearrangement from *trans* into *cis* – configuration (**26b**) could be noted after 1 day in solution. Obtained spectra of are described along with (**24**).

5.7.3 Dichloro-(κ^2 (C,O) - ((2-morpholinomethanone) benzylidene)-(1,3-bis (2,4,6-trimethylphenyl) 4, 5 – dihydroimidazol – 2 – ylidene) ruthenium (27a,b)

27 was prepared similar to **24**, using Neolyst **M3** (124 mg, 0.166 mmol, 1 eq), morpholino(2-vinylphenyl)methanone (**21b**) (55.4 mg, 1.5 eq) and 12 mL of degassed chloroform, The reaction mixture was allowed to stir overnight, whilst it turned dark green. After evaporation of the solvent, the residue was conducted to column chromatography. (silica, Cy:EtOAc 2+1 to 1+2 to CH_2Cl_2/MeOH 20:1 to pure MeOH). After elution of excess ligand and indenylidene, three different, intensively coloured products (brown, green, blue) could be isolated. They were assigned to excess Neolyst **M3** (TLC: CH_2Cl_2/MeOH 20:1; R_f = 0.52), *cis* – isomer (R_f = 0.43) and *trans* – isomer (R_f = 0.34) of desired product.[61]

NMR spectra were mainly compared in the carbene region, as aromatic and aliphatic region showed many impurities and indistinct peaks (compare figure 25).

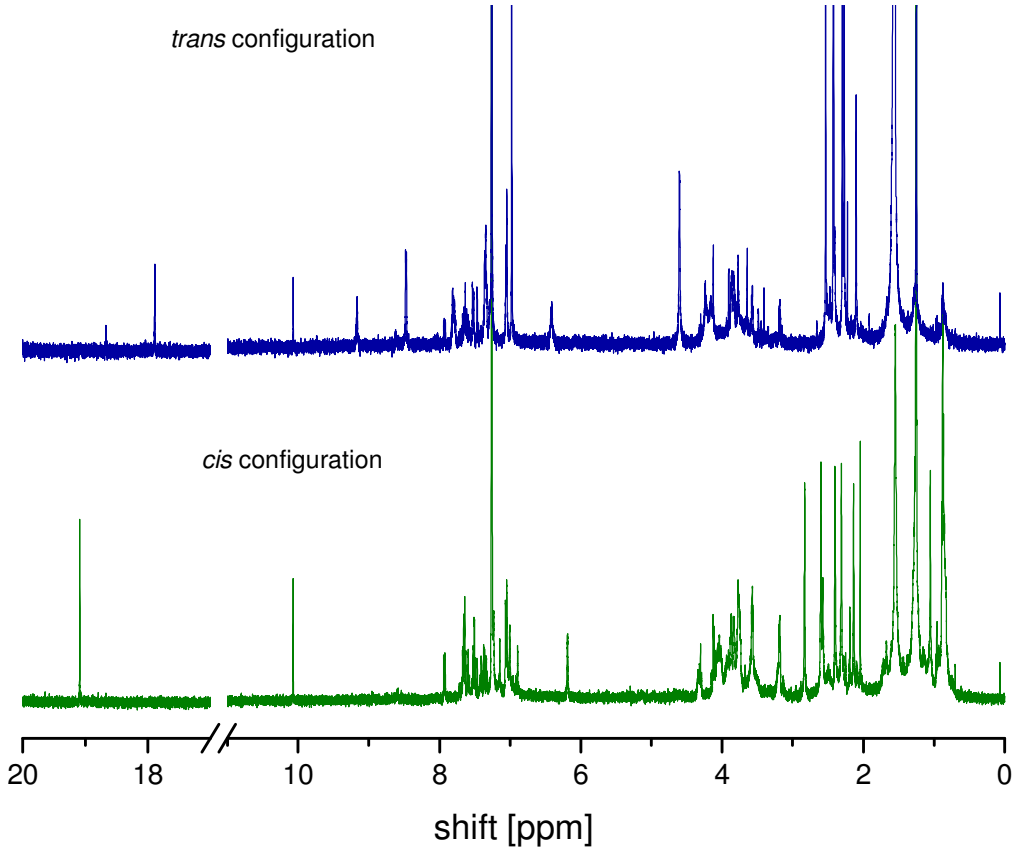

Fig. 25: 1H-NMR spectra of **15** Comparison of *trans*– and *cis*– isomere

[61] Kost, T.; Sigalov, M.; Goldberg, I.; Ben-Asuly, A.; Lemcoff, N. G. *J. Organomet. Chem.*, **2008**, *693*, 2200-2203.

5.7.4 Characterization of methylene-3-pheny-1H-indene (28)

TLC (silica, cyclohexane/ethyl acetate 3/1); R_f = 0.77

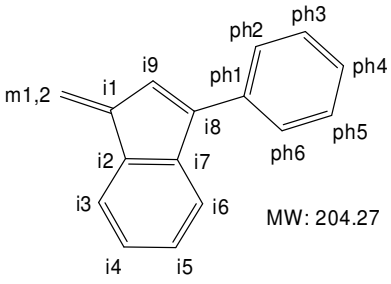

^{1}H-NMR (δ, 20°C, $CDCl_3$, 500 MHz): 7.69, 7.54 (2d, 2H, $i^{3,6}$); 7.61 (d, 2H, $ph^{2,6}$); 7.47 (t, 2H, $ph^{3,5}$); 7.39, 7.32 (2t,2H, $i^{4,5}$); 7.27 (t, 1H, ph^4); 6.63 (s, 1H, i^9); 6.13, 5.80 (2s, 2H, $m^{1,2}$).

^{13}C-NMR, **DEPT 135** (δ, 20°C, $CDCl_3$, 500 MHz): 146.9, 146.4, 142.4, 137.45, 135.6 ($5C_q$, $i^{1,2,7,8}$, ph^1); 128.9 ($2C_t$, $ph^{2,6}$); 127.8 ($2C_t$, $ph^{3,5}$); 128.3, 128.0, 126.8, 125.8, 120.4, 120.1 ($6C_t$, ph^4, $i^{3,4,5,6,9}$); 113.6 ($1C_s$, m).

5.7.5 (SPY-5-34)-Dichloro-(κ^2 (C,O) - (2-diethylamidebenzylidene) - (1,3-bis (2,4,6-trimethylphenyl) 4, 5 – dihydroimidazol – 2 – ylidene) ruthenium (29)

29 was prepared similar to **24**, using Neolyst **M3** (171.00 mg, 0.228 mmol, 1 eq), 2-vinyl-N,N-diethylbenzamide (**20b**) (70.20 mg, 1.5 eq) and 12 mL of degassed chloroform, The reaction mixture was allowed to stir for three days, whilst it turned green. After evaporation of the solvent the crude product was washed with n-pentane. The insoluble residue was filtered and subjected to column chromatography (silica, Cy:EtOAc 2+1 to 1+2 to CH_2Cl_2/MeOH 20:1 to pure MeOH). Fractions that were considered to contain product concentrated in vacuo, a dark green powder was obtained. Yield: 53.2 mg (35%). TLC (silica, solvent: CH_2Cl_2:MeOH 20:1) R_f = 0.50. ^{1}H-NMR spectrum showed three different carbene peaks, at 19.1, 18.64, and 17.91 ppm, Whereas in the aromatic region it was possible to assign product couplings, the aliphatic region was too crowded because of impurities. The following characterization contains only assigned peaks. The product was recrystallized by ether diffusion into a CH_2Cl_2 – solution of **29**.

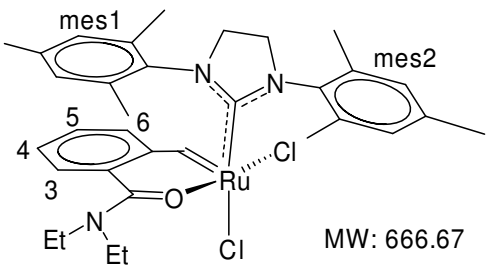

^{1}H-NMR (δ, 20°C, $CDCl_3$, 500 MHz): 19.1, 18.64, 17.91 (3 s, Ru=C*H*), 8.45 (bd, ph^3), 7.77, 7.60 (2bt, $ph^{4,5}$), 7.47 (bd, ph^6), 7.33, (s, 2H, mes1), 7.09, 6.96 (2s, mes2), aliphatic hydrogen couplings not assigned.

6 LIST OF ABBREVIATIONS

Ar	aryl
Ac	acetyl
Bu^t	*tert*-butyl
bz	benzyl
Cy	cyclohexane
DEDAM	diethyl 2,2-diallylmalonate
DME	dimethoxy ethane
DSC	differential scanning calorimetry
H_2IMes	N,N-bis(mesityl)-4,5-dihydro-imidazol-2-ylidene
hex	hexyl
L	ligand
M	molar, metal
MALDI-TOF MS	matrix assisted laser ion deposition – time of flight mass spectrometry
Mes	mesityl
MO	molecular orbital
MW	molecular weight, microwave
NHC	N-heterocyclic carbene
NMR	nuclear magnetic resonance
OLED	organic light emitting device
PDI	poly dispersity index
Ph	phenyl
ppm	parts per million
Pr^i	*iso*-propyl
Py	pyridine
RCM	ring closing metathesis
R_f	retention factor
ROMP	ring opening metathesis polymerization
SPY	square pyramide
TBAB	tetrabutylammonium bromide
TLC	thin layer chromatography

7 LIST OF FIGURES

8 LIST OF SCHEMES

9 LIST OF TABLES